their paper, Ng and Lim (1986)[19] made the line drawings of the carapace, chela, male abdomen, first and second male pleopods for the comparison with their new species, *S. insolita* from peninsular Malaysia. Diagnostic characters are given as follows. The dorsal surface of the carapace is flat, with the sharp epigastric and postorbital cristae; the external orbital tooth is flattened and lobular, with the convex outer margin the anterolateral margin is armed with three sharp teeth; the first two teeth are similar in shape and size, weakly curved and directed forward; the third tooth is subequal to, or slightly smaller than the preceding two teeth, straight and directed obliquely outward. The chelipeds are distinctly unequal, and the outer surface of the right (larger) palm is ornamented with dark reticulate pattern.

According to Naiyanetr (1998)[4], *Siamthelphusa improvisa* is known from Nakhon Si Thammarat, Phatthahung and Surat Thani Provinces, peninsular Thailand.

Acknowledgements

For the identification of some specimens and in getting the literature of Thai freshwater crabs, the authors are thankful Prof. Phaibul Naiyanetr of Chulalongkorn University, Bangkok, who is the pioneer and leading carcinologist in Thailand. This study was supported in part by a grant from the Nissan Science Foundation and by grants for Research on Emerging and Re-emerging Infectious Diseases from the Ministry of Health, Labor and Welfare of Japan (H18-Shinko-ippan-008 and H21-Shinko-ippan-004).

Literature

1) Rangsiruji, A., H. Sugiyama, Y. Morishima, Y. Kameoka, T. Donsakul, S. Binchai & P. Ketudat, 2006. A new record of *Paragonimus* other than *P. westermani* in southern Thailand. *SE Asian J. Trop. Med. Public Health*, **37** (Suppl. 3): 57-61.

2) Sugiyama, H., Y. Morishima, S. Binchai, A. Rangsiruji & P. Ketudat, 2007. New form of *Paragonimus westermani* discovered in Thailand: Morphological characteristics and host susceptibility. *SE Asian J. Trop. Med. Public Health*, **38** (Suppl. 1): 87-91.

3) Kemp, S., 1923. On a collection of river crabs from Siam and Annam. *J. Nat. Hist. Soc. Siam*, **6**: 1-42.

4) Naiyanetr, P., 1998. *Checklist of Crustacean Fauna in Thailand (Decapoda and Stomatopoda)*. Office of Environmental Policy and Planning, Bangkok, Thailand, 161 pp.

5) Bott, R., 1970. Die Süsswasserkrabben von Europoa, Asien, Australien und ihre Stammesgeschichite. Eine Revision der Potamoidea und Parathelphusoidea (Crustacea, Decapoda). *Abh. Senck. Nat. Ges.*, (526): 1-338.

6) Hilgendorf, F., 1882. Einige carcinologische Mittheilungen. *S. B. Ges. Nat. Freunde Berlin*, **1882**: 22-25.

7) Ng, P. K. L., 1986. *Phricotelphusa hockpingi* sp. nov., a new gecarcinucid freshwater crab from Perak, west Malaysia (Decapoda, Brachyura). *Crustaceana*, **51**: 270-276.

8) Naiyanetr, P., 1988a. New freshwater crab of Thailand: 2. Proc. 26th Conf. Fish. Sec., Kasetsart Univ., Bangkok, Thailand. (Not directly cited)

9) Naiyanetr, P., 1988b. Fresh water crabs in Thailand. In: Book published in memory of the Royal Cremation of Associate Professor Dr. Praphun Chitachumnong: 15 pp., 8 color pls., Mahidol Univ., Phaisalsipa Press, Bangkok, Thailand. (Not directly cited)

10) Ng, P. K. L. & P. Naiyanetr, 1993. New and recently described freshwater crabs (Crustacea: Decapoda: Brachyura: Potamidae, Gecarcinucidae and Parathelphusidae) from Thailand. *Zool. Verh.*, (284): 1-117.

11) Rathbun, M. J., 1905. Les crabes d'eau douce. *Nouv. Arch. Mus. Hist. Nat.*, Paris, (4), **7**: 159-323.

12) Bott, R., 1966. Potamiden aus Asien (*Potamon* Savigny und *Potamiscus* Alcock) (Crustacea, Decapoda). *Senck.*

THE JOURNAL OF BIOLOGICAL CHEMISTRY VOL. 285, NO. 10, pp. 7739–7751, March 5, 2010

A CD36-related Transmembrane Protein Is Coordinated with an Intracellular Lipid-binding Protein in Selective Carotenoid Transport for Cocoon Coloration*[S]

Received for publication, October 9, 2009, and in revised form, January 5, 2010 Published, JBC Papers in Press, January 6, 2010, DOI 10.1074/jbc.M109.074435

Takashi Sakudoh[‡], Tetsuya Iizuka[§], Junko Narukawa[¶], Hideki Sezutsu[§], Isao Kobayashi[§], Seigo Kuwazaki[¶], Yutaka Banno[‖], Akitoshi Kitamura[**], Hiromu Sugiyama[‡‡], Naoko Takada[‡], Hirofumi Fujimoto[‡], Keiko Kadono-Okuda[¶], Kazuei Mita[¶], Toshiki Tamura[§], Kimiko Yamamoto[¶], and Kozo Tsuchida[‡1]

From the [‡]Division of Radiological Protection and Biology, National Institute of Infectious Diseases, Shinjuku, Tokyo 162-8640, the [§]Transgenic Silkworm Research Center and [¶]Insect Genome Research Unit, National Institute of Agrobiological Sciences, Tsukuba, Ibaraki 305-8634, the [‖]Genetic Resources Technology, Kyushu University, Fukuoka, Fukuoka 812-8581, the [**]Life Science Division, Fuji Chemical Industry Co., Ltd., Nakaniikawa, Toyama 930-0397, and the [‡‡]Department of Parasitology, National Institute of Infectious Diseases, Shinjuku, Tokyo 162-8640, Japan

The transport pathway of specific dietary carotenoids from the midgut lumen to the silk gland in the silkworm, *Bombyx mori*, is a model system for selective carotenoid transport because several genetic mutants with defects in parts of this pathway have been identified that manifest altered cocoon pigmentation. In the wild-type silkworm, which has both genes, *Yellow blood* (*Y*) and *Yellow cocoon* (*C*), lutein is transferred selectively from the hemolymph lipoprotein to the silk gland cells where it is accumulated into the cocoon. The *Y* gene encodes an intracellular carotenoid-binding protein (CBP) containing a lipid-binding domain known as the steroidogenic acute regulatory protein-related lipid transfer domain. Positional cloning and transgenic rescue experiments revealed that the *C* gene encodes *Cameo2*, a transmembrane protein gene belonging to the CD36 family genes, some of which, such as the mammalian *SR-BI* and the fruit fly *ninaD*, are reported as lipoprotein receptors or implicated in carotenoid transport for visual system. In *C* mutant larvae, Cameo2 expression was strongly repressed in the silk gland in a specific manner, resulting in colorless silk glands and white cocoons. The developmental profile of *Cameo2* expression, *CBP* expression, and lutein pigmentation in the silk gland of the yellow cocoon strain were correlated. We hypothesize that selective delivery of lutein to specific tissue requires the combination of two components: 1) CBP as a carotenoid transporter in cytosol and 2) Cameo2 as a transmembrane receptor on the surface of the cells.

All organisms exposed to light contain carotenoids, which are yellow to red C_{40} hydrophobic isoprenoid pigments. Carotenoids play pivotal roles in living organisms as precursors of vitamin A, antioxidants, and colorants (1). Their potential roles in medicine have recently been investigated. For example, macular accumulation of the carotenoids lutein and zeaxanthin is associated with a decreased risk of age-related macular degeneration (2), the leading cause of blindness in the developed world. Although plants, certain fungi, and bacteria synthesize carotenoids, animals appear to be incapable of synthesizing these molecules *de novo*. Therefore, animals must acquire carotenoids from dietary sources, and subsequently transport them to cells of target tissues.

The delivery of lipids, including carotenoids, to cells can be divided into three categories: 1) enzyme-mediated processes, such as the action of lipoprotein lipase on very low density lipoproteins, which converts a lipoprotein-bound lipid, triacylglycerol, into a water-soluble product, fatty acid, which diffuses into cells and leaves behind in the blood a lipoprotein product depleted in triacylglycerol (3); 2) receptor-mediated endocytosis, such as the uptake of low density lipoproteins by low density lipoprotein receptor, in which the entire lipoprotein particle is taken into the cell and metabolized (4); and 3) the delivery of specific lipids to specific tissues devoid of lipoprotein degradation, called selective lipid transport, such as the delivery of cholesterol ester from high density lipoprotein (HDL)[2] to the adrenal gland (5). The first two mechanisms have been extensively studied in vertebrates. However, the third mechanism, which clearly occurs in both vertebrates and invertebrates, is poorly understood.

In the domesticated silkworm, *Bombyx mori*, previous works have demonstrated the existence of tissue-specific delivery of

* This work was supported by the Kieikai Research Foundation (Japan), the Futaba Electronics Memorial Foundation (Japan), a grant-in-aid for scientific research from the Japan Society for the Promotion of Science, the Insect Technology Project of the Ministry of Agriculture, Forestry and Fisheries (Japan), and the National Bioresource Project (Silkworm) of the Ministry of Education, Culture, Sports, Science, and Technology (Japan).

[S] The on-line version of this article (available at http://www.jbc.org) contains supplemental "Experimental Procedures," Tables S1–S3, and Figs. S1–S5.

The nucleotide sequence(s) reported in this paper has been submitted to the GenBank™/EBI Data Bank with accession number(s) AB515345–AB515347.

[1] To whom correspondence should be addressed: 1-23-1 Toyama, Shinjuku, Tokyo 162-8640, Japan. Tel.: 81-3-5285-1111 (ext. 2421); Fax: 81-3-5285-1194; E-mail: kozo@nih.go.jp.

[2] The abbreviations used are: HDL, high density lipoprotein; *C*, *Yellow cocoon*; Cameo, *C* locus-associated membrane protein homologous to a mammalian HDL receptor; CBP, carotenoid-binding protein; SR-BI, scavenger receptor class B type I; RT, reverse transcriptase; SNP, single nucleotide polymorphism; START, steroidogenic acute regulatory protein-related lipid transfer; UAS, upstream activating sequence; IV0, day 0 of the fourth instar; V0, day 0 of the fifth instar; W0, day 0 of the wandering stage; *Y*, *Yellow blood*; HPLC, high-performance liquid chromatography; EGFP, enhanced green fluorescent protein.

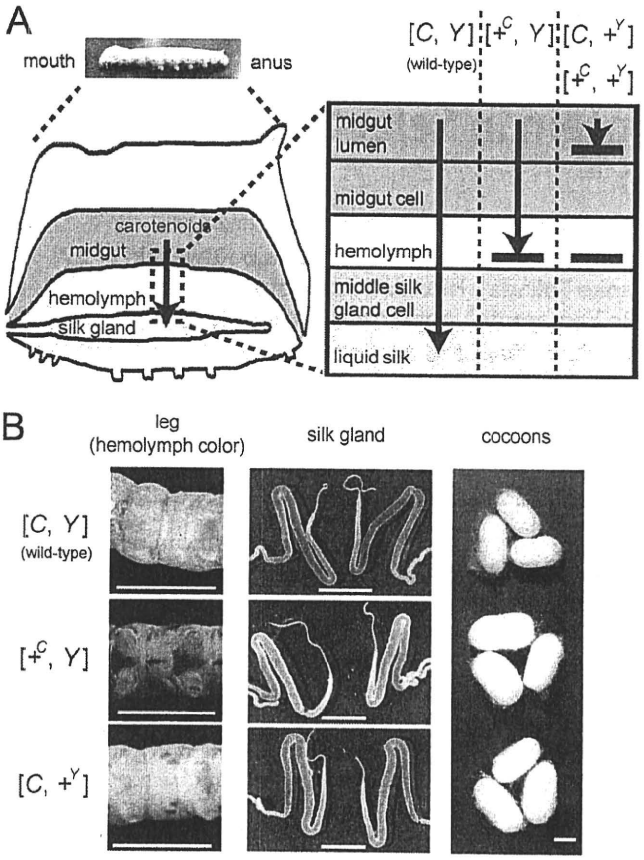

FIGURE 1. **Transport of lutein by the *Yellow cocoon* (*C*) gene and the *Yellow blood* (*Y*) gene.** *A*, schematic representation of the functions of the *C* and *Y* genes in the carotenoid transport system of the silkworm. $+^{C}$ and $+^{Y}$ represent a recessive allele of the *C* and *Y* genes, respectively. *B*, color phenotype of the hemolymph, silk gland, and cocoons. The hemolymph color is visible on the abdominal legs where the skin is relatively transparent. The silk glands are paired organs. The c10, c05, and FL501 ($+^{Y}$) strains were used as the genotypes of [*C*, *Y*], [$+^{C}$, *Y*], and [*C*, $+^{Y}$], respectively. The silkworm with the genotype of [$+^{C}$, $+^{Y}$] exhibits colorless hemolymph and produces white cocoons, similar to [*C*, $+^{Y}$]. Legs were at day 3 of the fifth larval instar (V3). Silk glands were at day 0 of the wandering stage (W0). The lutein content of the middle silk gland of [*C*, *Y*] was about 30-fold higher than that of [$+^{C}$, *Y*] (data not shown). The *black* color of the larval skin of the c05 strain was due to the larval marker gene, p^{S}. *Scale bar*, 1 cm.

specific carotenoids (6–9). The wild-type silkworm feeds on carotenoid-rich mulberry leaves in the larval stage. Carotenoids are then absorbed into the midgut epithelium, transferred to the hemolymph lipoprotein, lipophorin, and accumulated in the middle silk gland, resulting in yellow hemolymph and the formation of a yellow cocoon (Fig. 1, *A* and *B*). Lipophorin facilitates lipid transport in insects in a selective manner (10). Over the 4000 year history of sericulture, several mutants have been noted that produce white cocoons due to defect in carotenoid transport (11). Among these are mutants in the selective transport of carotenoids from lipophorin to the middle silk gland. Molecular cloning of the genes responsible for these mutants therefore provides tools to determine the molecular mechanism of selective carotenoid transport.

The *Yellow blood* (*Y*) gene on chromosome 2 of *B. mori* controls transport of carotenoids from the midgut lumen to the midgut epithelium and from the lipophorin to the middle silk gland cells (Fig. 1*A*) (7–9). We have reported previously that the *Y* gene encodes an intracellular carotenoid-binding protein (CBP) (12), which was identified based on a combination of expression analysis (12, 13), restriction fragment length mapping (14), genomic sequence analysis (15, 16), and transgenic rescue of phenotype (16). CBP is a 33-kDa protein containing a lipid-binding domain known as the steroidogenic acute regulatory protein-related lipid transfer (START) domain (17). CBP is expressed in the midgut, the middle silk gland, testis, and ovary in the dominant *Y* allele strain ("*X* allele strain" represents the strain harboring the homozygous *X* allele), producing yellow cocoons. In *Y* mutants homozygous for the recessive $+^{Y}$ allele, genomic deletion of the *CBP* gene leads to complete absence of the CBP protein. The midgut epithelium, therefore, poorly absorbs carotenoids, resulting in colorless hemolymph, colorless middle silk gland, and white cocoons (Fig. 1*B*).

The *Yellow cocoon* (*C*) gene on chromosome 12 controls transport of carotenoids, mainly lutein, from lipophorin to the middle silk gland cells (Fig. 1*A*) (11, 18). The middle silk glands of the *C* mutants, homozygous for the recessive $+^{C}$ allele, have a defect in the cellular uptake of lutein and are, therefore, colorless even in the presence of yellow hemolymph mediated by the dominant *Y* allele of the *Y* gene, resulting in white cocoons (Fig. 1*B*). Selective transport of lutein from lipophorin to middle silk gland cells by the dominant *C* allele requires the *Y* allele (19, 20). Thus, molecular cloning of the *C* gene was expected to offer a novel molecular component that facilitates selective transport of lutein in coordination with CBP in middle silk gland cells.

In the present study, the *C* gene was cloned using a positional cloning method, resulting in identification of Cameo2 (C locus associated membrane protein homologous to a mammalian HDL receptor-2). Cameo2 belongs to the CD36 family, including scavenger receptor class B type I (SR-BI), a transmembrane receptor of mammalian HDL (5). A molecular pathway for selective lutein transport in the body of the silkworm by a combination of Cameo2 and CBP is proposed.

EXPERIMENTAL PROCEDURES

Silkworm Strains—The c04, c05, c10, c11, c43 (*Pk*), e09, FL501 ($Y/+^{Y}$), and FL501 ($+^{Y}/+^{Y}$) strains have been preserved at the silkworm stock center of Kyushu University, Fukuoka, Japan. The number 925 and w1-pnd strains have been preserved in the National Institute of Agrobiological Sciences, Ibaraki, Japan. The N4 strain has been preserved at the National Institute of Infectious Diseases, Tokyo, Japan. The Kinshu X Showa F1 hybrids were a generous gift from Dr. Toru Shimada (University of Tokyo, Tokyo, Japan). The larvae were reared on mulberry leaves or an artificial diet made from mulberry leaves (Nihon Nosan Kogyo Co., Yokohama, Japan). Data regarding the origin, genotype, and phenotype of these strains are summarized in supplemental Table S1. The first days corresponding to the developmental stages of the third to fourth larval ecdysis, the fourth to fifth larval ecdysis, and wandering, a characteristic behavior with enhanced locomotory activity just before spinning cocoons, were designated as IV0, V0, and W0, respectively.

Crossing and Genomic Extraction for Mapping of the C Gene—Two silkworm strains, c11 (*C*/*C*, *Y*/*Y*, yellow cocoon with yel-

low hemolymph) and number 925 ($+^C/+^C$, *Y/Y*, white cocoon with yellow hemolymph) were used. Single-pair crosses between number 925 and c11 produced F1 offspring. As female recombination is uncommon in *B. mori* (21), BF1 progeny from the single-pair cross between female number 925 and males of F1 (number 925 X c11) were used for recombination mapping. The number of single-pair matings for BF1 progeny was 18. Each of the total of 1775 BF1 individuals was named, phenotypically recorded, and subjected to genomic DNA extraction using DNAzol Reagent (Invitrogen). None of the BF1 individuals analyzed showed colorless hemolymph.

Mapping Using Single Nucleotide Polymorphism (SNP) Markers—For mapping using the BF1 progeny, PCR primer sets were generated at each position on chromosome 12, and primer sets with that the PCR products showed polymorphism between parents were used for SNP markers. The PCR primers used for SNP analysis are listed in supplemental Table S2. The PCR products treated with ExoSAP-It (U. S. Biochemical Corp.) were subjected to direct sequencing.

RNA Extraction—Total RNA was isolated from tissues washed in insect saline (20 mM sodium phosphate buffer, 150 mM sodium chloride, pH 6.7) with TRIzol reagent (Invitrogen). Before addition to TRIzol reagent, the silk gland and midgut were frozen in liquid nitrogen and broken into fine pieces. The other tissues were syringe-homogenized in TRIzol reagent.

Comparison of the Cameo1 and Cameo2 cDNA Sequences between the C and $+^C$ Allele Strains—*Cameo1* and *Cameo2* were amplified from the middle silk gland of each strain via reverse transcription (RT)-PCR and directly sequenced. The PCR primers used for each gene and strain are listed in supplemental Table S3.

Data Base Search for Cameo1 and Cameo2 Homologs in the Silkworm—The silkworm genome contained 13 annotated genes homologous to *Cameo1* and *Cameo2*, which were retrieved from the KAIKObase system through a keyword search using "CD36" as the query. The TBLASTN program was used to search for all genes homologous to *Cameo1* and *Cameo2* in the silkworm genome sequence (22) and EST data base (23) with a cutoff *E* value of 5×10^{-3} and the results did not include any others besides these 13 genes. One of these homologous genes, *SNMP1*, has been cloned (24), and recently 10 of them were reported and named by independent data base searches (25, 26). We use in this paper the same names for the total 11 genes and term the other two genes, BGIBMGA13436 and BGIBMGA13438 in the China gene model ("BGIBMGA" is a prefix for gene name), SCRB14 and SCRB15, respectively.

Phylogenetic Analysis of the Protein Sequences Homologous to Cameo1 and Cameo2—Alignment of the hypothetical protein sequences was performed using Clustal W2 (27). A phylogenetic tree was then constructed with the neighbor-joining method using Clustal X2 (27).

Northern Blotting—For *Cameo2*, a ^{32}P-labeled riboprobe was synthesized from the N-0394 EST clone. The insert of N-0394 contained the 3′ part (1016 bp) of the open reading frame and the 5′ part (1209 bp) of the 3′-untranslated region of *Cameo2*. No silkworm repetitive sequence was found in the insert. Total RNA was electrophoresed on 1% agarose gels containing formaldehyde and transferred onto Hybond N^+ membrane (GE Healthcare UK). Hybridization was performed with Ultrahyb (Ambion, Austin, TX).

RT-PCR Analysis of Tissue Distribution of Cameo1, Cameo2, and rpL3—Primer1-1 (5′-CTGAAAGTGGAGCAGTTGGGTCCTTACG-3′) and Primer1-4 (5′-CGGACACCTTGACGACCCTGGGCTGGTG-3′) for *Cameo1*, Primer2-3 (5′-GGACCAGGTCACCGGCATGAACCCGGATC-3′) and Primer2-2 (5′-CGTCCTCAGCTCCGAAATGATTTTTGGATC-3′) for *Cameo2*, and Primer-rpL3-real-cDNA1 (5′-TTCCCGAAAGACGACCCTAG-3′) and Primer-rpL3-real-cDNA2 (5′-CTCAATGTATCCAACAACACCGAC-3′) for *rpL3* were used.

Analysis of Carotenoid Composition of the Middle Silk Gland—Samples of the middle silk gland cut into small pieces less than 1 mm length (~200 mg) were transferred into a glass centrifuge tube with 5 ml of distilled water and 2 g of glass beads (1 mm diameter) as agitating aid were added. After heating at 90 °C for 15 min, eluate was collected. 5 ml of 80% ethanol with butylhydroxytoluene as an antioxidizing agent at a concentration of 10 μg/ml was added to the residue, followed by heating at 90 °C for 10 min with vortexing at intervals. The eluate was then collected. Extraction with 80% ethanol was repeated three times. 3 ml of 100% ethanol with butylhydroxytoluene was added to the residue, followed by heating at 90 °C for 10 min with vortexing at intervals. The eluate was then collected. Extraction with ethanol was repeated until the residue became colorless. All of the collected extracts were pooled, and ethanol was evaporated. 1 g of sodium sulfate decahydrate was then added followed by extraction three times with 5 ml of petroleum ether. 9 ml of acetone was added to the aqueous layer, then extracted with 5 ml of petroleum ether three times. The organic phase was dried over anhydrous sodium sulfate and evaporated. The residue was resolved in acetone and used for carotenoid analysis by high performance liquid chromatography (HPLC). A reverse-phase column (YMC carotenoid 5 μm (4.6 × 250 mm); Waters Co., Milford, MA) was used under the following conditions: temperature, 25 °C; flow rate, 1 ml/min; mobile phase, A, methanol; B, *t*-butylmethylether; C, 1% (v/v) aqueous phosphoric acid; a 15-min linear gradient from 81% A, 15% B, 4% C to 66% A, 30% B, 4% C; an 8-min linear gradient to 16% A, 80% B, 4% C, a 4-min hold at 16% A, 80% B, 4% C, then back to 81% A, 15% B, 4% C, and an 8-min hold at 81% A, 15% B, 4% C.

Quantification of Transcripts by Real Time PCR—Single-stranded cDNAs from various tissue samples were synthesized from total RNAs with Superscript III reverse transcriptase (Invitrogen) with oligo(dT) primer, and treated with RNase H (Takara, Kyoto, Japan). Quantification of transcripts was carried out by real time PCR using these cDNAs as templates with LightCycler FastStartDNA MasterPLUS SYBR Green I (Roche) and LightCycler DX400 (Roche). The primer pairs used for detection of *Cameo1*, *Cameo2*, *CBP*, and *rpL3* were Primer1-1 and Primer1-6 (5′-CGCCACAGTCGCTATTATAGGGTTGATGC-3′); Primer2-19 (5′-AGTGTTAGAGGAGGTGCACCAGCTC-3′) and Primer2-16 (5′-CAGTCCGTTTTGAACCCCACTCTCC-3′); PrimerCBP-1 (5′-ATGGCCGACTCTACGTCGAAAAGCG-3′) and PrimerCBP-18 (5′-GCCTTCAACTTTCCTTGACTCCACGACG-3′); and Primer-rpL3-real-cDNA1 and Primer-rpL3-real-cDNA2, respectively. For *Cameo1*, *Cameo2*, and *rpL3*, absence of mutation in the anneal-

ing sites of these primers among the analyzed strains was confirmed (supplemental Fig. S2). Serial dilutions of plasmids containing the cDNA sequences were used as standards. Transcript levels of *Cameo1*, *Cameo2*, and *CBP* were normalized with the level of the *rpL3* transcript in the same samples, as described previously (28).

Analysis of F1 SNPs of Cameo1 and Cameo2—The cDNA sequences of *Cameo1* and *Cameo2* of each parental strain were aligned (supplemental Fig. S2). Then primer pairs, Primer1-3 (5′-GAGGGCGTTCGGTACGCGGCCAACGACTC-3′) and Primer1-2 (5′-CTGGATCTTGCTGGGGTAGTACGGGTC-3′) for *Cameo1*, Primer1-25 (5′-TATCAACAACGTGTTGC-CGGACC-3′) and Primer1-16 (5′-GTGAGGGTGTAGAGC-GCGTATG-3′) for *Cameo1*, Primer2-19 and Primer2-16 for *Cameo2*, and Primer2-21 (5′-TCCTTACCGTTACCAGGAG-CATAG-3′) and Primer2-20 (5′-GCGGTTATAACGTCAAT-GGTTGTG-3′) for *Cameo2* were designed according to the conserved nucleotide sequence for PCR amplification of the cDNA and genomic DNA of the parental and F1 strains, and the PCR products by these primer pairs were directly sequenced with Primer1-2, Primer1-25, Primer2-18 (5′-TTG-GAGCATTCGCCGTCG-3′), and Primer2-21, respectively.

Western Blotting—A rabbit polyclonal antibody against Cameo2 was raised against the synthetic peptide (C-)NGLKY-NKYEVNERS (amino acids 295–308, corresponding to the putative extracellular domain (Fig. 3*B*)) coupled to keyhole limpet hemocyanin and affinity purified by Operon Biotechnologies (Tokyo, Japan). For Western blotting analysis of the membrane fraction, 100 pieces of the silk gland of each strain on the day 0 of the wandering stage (W0) was homogenized in ice-cold insect saline containing a protease inhibitor mixture (Protease Inhibitor Mixture Set III, EDTA-free, Calbiochem, San Diego, CA) using a Polytron homogenizer. The homogenate was centrifuged at 800 × *g* for 10 min, and the supernatant was filtered through cheesecloth and centrifuged at 1,000 × *g* for 10 min. The membranes were then pelleted by centrifugation at 100,000 × *g* for 1 h and resuspended in 20 mM Tris-HCl, 150 mM NaCl, 2 mM $CaCl_2$, 0.1 mM phenylmethylsulfonyl fluoride, pH 7.4, at a concentration of 10 mg of protein/ml. Then, the same volume of 80 mM *n*-octylglucoside was added for solubilization. After mixing for 1 h, insoluble material was removed by centrifugation at 100,000 × *g* for 1 h. The concentration of *n*-octylglucoside in soluble extract was adjusted to 5 mM by addition of 7 volumes of 20 mM Tris-HCl buffer, and centrifuged at 100,000 × *g*, 1 h to collect precipitate. The pellet was resuspended again in 20 mM Tris-HCl, 150 mM NaCl. The protein concentration was determined with the Bradford method (Protein Assay solution; Bio-Rad). Then, 25 μg of protein was separated by SDS-PAGE, transferred to polyvinylidene difluoride membrane, and probed with the anti-Cameo2 antibody and a sheep anti-rabbit IgG-conjugated alkaline phosphatase (Jackson ImmunoResearch Laboratory, West Grove, PA). The signals were detected by AP-conjugate Substrate Kit (Bio-Rad).

Immunohistchemistry—Cross-sections of the middle silk gland from the region of "MSG-3" in Fig. 5*C* were deparaffinized in xylene, rehydrated through graded ethanol solutions, and quenched with a 30-min immersion in 0.3% hydrogen peroxide in methanol. Sections were blocked for 30 min in normal goat serum in phosphate-buffered saline, and incubated with the Cameo2 antibody (at 1:1000 dilution) used for the Western blotting experiment overnight at 4 °C. Sections were rinsed in phosphate-buffered saline, and incubated for 30 min with a biotinylated goat anti-rabbit IgG (at 1:200 dilution). The slides were developed using the ABC Vectastain Elite kit (Vector Labs, Burlingame, CA) following the manufacturer's instructions. The slides were counterstained in Mayer hematoxylin.

Silkworm Transgenesis—We first attempted to produce the nondiapausing strain with the phenotype of yellow hemolymph and white cocoons. The number 925 strain of the genotype [Y, $+^{C}$] was crossed with the w1-pnd strain, a nondiapausing strain with the genotype [$+^{Y}$, $+^{C}$] used for transgenesis of *B. mori* (29). By sib mating of the progeny, a nondiapausing strain with the phenotype of yellow hemolymph and white cocoons, termed w1-pnd-925, was established.

For transgenic expression of Cameo2 in the w1-pnd-925 strain by the binary GAL4/upstream activating sequence (*UAS*) system (30), *Cameo2* was amplified by RT-PCR from the middle silk gland of the N4 strain with Primer2-13 (5′-ATGCTCTAG-ATTCCTTGTGATAATCGCGGC-3′) and Primer2-10 (5′-ATGCTCTAGACATACGGACTCATTCCAATG-3′), both of which have an XbaI site. The PCR product was subcloned into the pGEM T-vector, and the subcloned product was digested with XbaI. The fragment was ligated into the vector *pBacMCS-[UAS-3xP3-EGFP]* (16) previously digested with BlnI. The resulting effector construct *pBacMCS[UAS-Cameo2-3xP3-EGFP]* was confirmed by DNA sequencing. For the effector strains, the effector construct and the helper plasmid, pHA3PIG (29), were injected into preblastoderm embryos of the w1-pnd-925 strain at a concentration of 0.2 mg/ml. After sib selection based on the presence of EGFP fluorescence in the eye by the *3xP3-EGFP* gene, G1 male moths of a UAS-Cameo2 (UAS) line with the phenotype of yellow hemolymph and white cocoons were crossed with females of the Ser1-GAL4 (GAL4) line with the phenotype of colorless hemolymph and white cocoons, which drives target gene expression in the middle silk gland and has a marker fluorescence in the eye by the *3xP3-DsRed* gene (31). Because the transgene was supposed to be homozygous in the GAL4 line, the progeny of the cross between the UAS line and GAL4 line showed two different marker phenotypes of eye color: both DsRed- and EGFP-positive, GAL4/UAS line (Ser1-GAL4(+), UAS-Cameo2(+)); and only DsRed-positive, GAL4 line (Ser1-GAL4(+), UAS-Cameo2(−)). Data from the individuals exhibiting colorless hemolymph in the larval stage, which had colorless silk glands and produced white cocoons, were not presented in Fig. 7, *B–E*. Experimental procedures for determination of the *Cameo1* and *Cameo2* cDNA sequence and Southern blotting are described under supplemental data.

RESULTS

Mapping of the C Locus—To identify a candidate physical region for the *C* locus, we performed genetic linkage analysis using SNP markers (32, 33). First, the *C* locus was roughly mapped with 75 BF1 individuals, and the *C*-linked region was narrowed to the 1.94 Mb range on chromosome 12 between two SNP markers, 12-055 and 12-056 (Fig. 2*A*). Then, novel

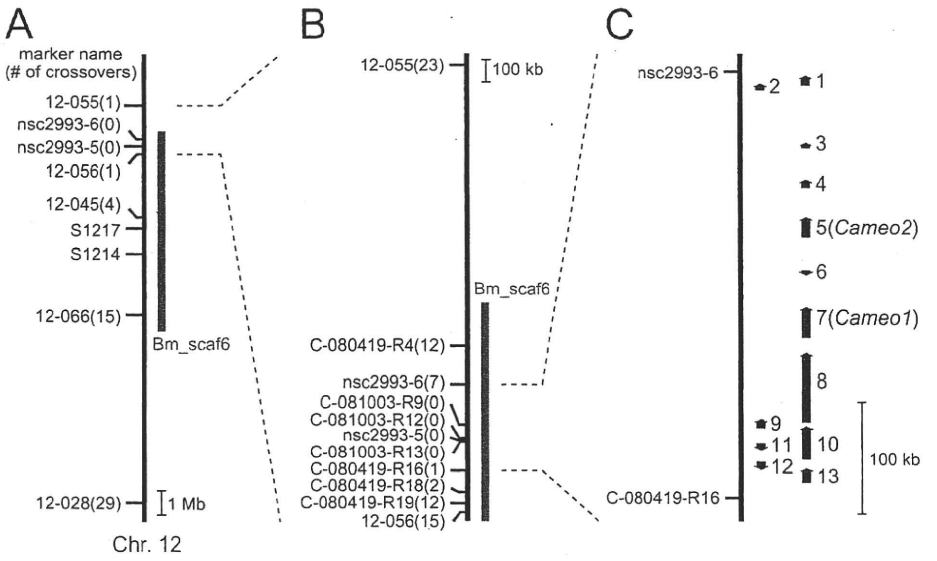

FIGURE 2. **Mapping of the *C* gene on the chromosome 12.** *A*, rough mapping with 75 individuals. *Small horizontal lines* on the *vertical bars* of chromosome 12 denote the positions of crossover events with the name of the SNP maker and the number of recombinants. Recently, Li and colleagues (63) independently showed that the *C* locus was closer to SSR marker S1217 than S1214, consistent with our results. *B*, finer mapping with 1700 individuals. *C*, physical map of chromosome 12 near the *C* locus with the predicted gene. *Vertical arrows* indicate the orientation and relative size of the 13 putative genes predicted by the China gene model (22). *1*, BGIBMGA010481 (SMAD homolog); *2*, BGIBMGA010480 (unknown); *3*, BGIBMGA010479 (unknown); *4*, BGIBMGA010478 (similar to the CG7231 gene of *D. melanogaster*, whose molecular function is unknown); *5*, BGIBMGA010477 (*Cameo2*); *6*, BGIBMGA010502 (unknown); *7*, BGIBMGA010476 (*Cameo1*); *8*, BGIBMGA010475 (dynein heavy chain homolog); *9*, BGIBMGA010474 (dynein heavy chain homolog); *10*, BGIBMGA010473 (dynein heavy chain homolog); *11*, BGIBMGA010503 (homolog of SprT-like metalloproteases with zinc finger domain); *12*, BGIBMGA010504 (tetraspanin homolog); *13*, BGIBMGA010472 (similar to muscle-specific protein 300, involved in cytoskeleton organization).

primer sets were designed in the narrowed range, and finer mapping was performed with 1700 BF1 individuals. As a result, the *C*-linked region was further narrowed to the 375-kb range between two SNP markers, nsc2993-6 and C-080419-R16, which was on one scaffold, Bm_scaf6 (Fig. 2*B*).

Candidates for the C Gene—Thirteen genes were predicted within the narrowed region by the China gene model at KAIKObase (22) (Fig. 2*C*). Among them, two genes were found to encode proteins homologous to SR-BI, a mammalian transmembrane cell surface receptor for HDL (5, 34–36). SR-BI mediates cellular uptake of cholesteryl ester from HDL in a selective manner. SR-BI was proposed to form a hydrophobic channel along which cholesteryl esters migrate (37). Furthermore, mutants of the *ninaD* gene, a homolog of SR-BI in the fruit fly *Drosophila melanogaster*, was reported to affect carotenoid uptake in gut for visual chromophore synthesis (38–40), and SR-BI was also implicated in cellular carotenoid absorption (41–44). Therefore, we considered these two genes to be strong candidates for the *C* gene, and designated the gene nearer the SNP marker C-080419-R16 *Cameo1* and the other *Cameo2*.

Characterization of the Cameo1 and Cameo2 Sequences—We determined each cDNA sequence containing the full-length of the open reading frame of *Cameo1* and *Cameo2* from a *C* allele strain. *Cameo1* and *Cameo2* span a region of 120 kb in the Bm_scaf6, and are composed of 11 and 10 exons, respectively (Fig. 3*A*). The deduced amino acid sequence indicated that Cameo1 and Cameo2 are a 56.2-kDa protein of 495 amino acids and a 56.0-kDa protein of 494 amino acids, respectively (Fig. 3*B*). The degree of identity between Cameo1 and Cameo2 is 28%. Cameo1 and Cameo2 share 32 and 26% amino acid identity, respectively, with the human SR-BI and 32 and 31% identity, respectively, with the fruit fly NinaD. TMHMM version 2.0 (45), software for prediction of transmembrane helices, predicted that both gene products are comprised of a large extracellular loop, anchored to the plasma membrane on each side by transmembrane domains adjacent to short cytoplasmic N-terminal and C-terminal domains (Fig. 3*B*). SignalP 3.0-HMM (46), a program for prediction of signal peptide, predicted that the N termini of Cameo1 and Cameo2 are signal peptides with a probability of 29 and 95%, respectively. The cleavage site with maximum probability was near the C terminus of the N-terminal putative transmembrane domain in Cameo1 and Cameo2, respectively (Fig. 3*B*, *arrow*). Therefore, we tentatively propose that Cameo1 and Cameo2 are single- or double-pass transmembrane proteins (Fig. 3*C*). It could be noted that the existence of the N-terminal transmembrane helix in SR-BI homologs, CD36 family genes, has been a matter of debate (5, 47), and some of them were similarly predicted to have a single- or double-pass transmembrane structure at various ratios (Fig. 3*C*).

There are 13 other genes homologous to *Cameo1* and *Cameo2* in the silkworm genome data base (22). These genes were distributed or tandemly positioned in several chromosomes (Fig. 3*D*). No homologous genes other than *Cameo1* and *Cameo2* were found on chromosome 12, where the *C* locus lies. The phylogenetic tree of these silkworm genes was generated with the CD36 family genes from insects and mammals (Fig. 3*E*). As indicated in a previous study in Dipterans (48), the insect genes could be largely divided into three groups, and *Cameo1* and *Cameo2* fall into the Group 2. Group 2 contains functionally characterized genes of *D. melanogaster*. *Santa maria* is implicated in cellular uptake of carotenoids in extraretinal neural cells in heads (40), *crq* is required for efficient phagocytosis of apoptotic cells (49), and *pes* was identified as a host factor required for the uptake of mycobacteria (50). The orthologous relationships of the Group 2 genes were not clear. SNMP in Group 3 is required for chemoreception of (*Z*)-11-octadecenyl acetate in olfactory neurons of *D. melanogaster* (24, 51, 52). The mammalian homologs formed a distinct group. CD36 is implicated in cellular uptake of long-chain fatty acids (53).

Comparison of the Nucleotide Sequences of Cameo1 and Cameo2 between the C and $+^C$ Allele Strains—Southern blotting analysis suggested that the silkworm has a single copy of

the *Cameo1* and *Cameo2* genes irrespective of the genotype of the *C* gene (supplemental Fig. S1). Then, to examine the relationship between the *C* gene with *Cameo1* and *Cameo2*, we compared the mRNA sequences of *Cameo1* and *Cameo2* among three *C* allele strains and four $+^{C}$ allele strains (supplemental Fig. S2). The mRNA sequences of *Cameo1* and *Cameo2* were well conserved and absent of indels and premature stop codons, whereas one nonsynonymous mutation in Cameo1

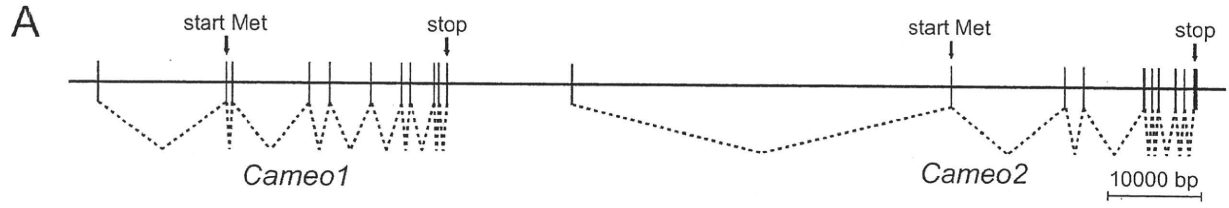

B

```
Cameo1    1: MKMVSSGV-KSG-LFMGFGSAL-VLIGAIVV-VYWPSIFMAQLQRMMILSPISISFGIWQ 56
Cameo2    1: --MRG-GLLRWRSLWICGG-ALLALS-AFVAALTWGAIFDSAFGSQLALIPDSRSFMRWL 55

Cameo1   57: ETPIPMYLECYMFNITNADKILAKEDVILKVEQLGPYVFRESHSKVNLTWN-DNSTITFY 115
Cameo2   56: EPDVPIFFDIYMFNWTNPERFPEEKPN-F--EEIGPYRYQEHRRHVNISWHPENGTIGYR 112

Cameo1  116: NQREWHFDQNLSKGSLSDEIIS-INFIIATVAYIVRHQPRVVKVSVDVFLRMFHDDLF-L 173
Cameo2  113: TLRSWVWDESSV-GSQ-DDIITTIDVITASAIYQARFSGFIEQKIVSLTLTSSQHTKVSV 170

Cameo1  174: KANVSSWLFEGIEDPVLEMAQKFPDLPLNI-PY-DKFGWEYERNGSREFDGSFI-MNT-G 229
Cameo2  171: TARASEFLFEGMEDPLLNLAKLMPASVRGGAPAIDRFGWEFSRNNTDT-DG-YMEV-TSG 227

Cameo1  230: AADFSRL-GNIEL-WKYSPRTVFRDH-CGDVKGSTGELWAPELGQPELFV-FASDICTYL 285
Cameo2  228: TRDG--LPGQI-LRWNYQDHIPFYDGECSKLSGSAGEYIPRNLTEDSKLTMYVPDLCRTV 284

Cameo1  286: TLHKKEDVLIENIEGVRYAANDSLFDNGHKYPAMACYCDEVRDRDCVPPGALNVSLCRLG 345
Cameo2  285: NMEFVESGVQNGLKYNKYEVNERSFDNSSTSPENTCFCKG----ECAWGGVMNVSACRFG 340

Cameo1  346: APAFVSQPHFLDADPYYPSKIQGLLPQEE-HRFSLALEM-FTGMPLAVSAQLQINLLIRD 403
Cameo2  341: SPAFITLPHFLHGDPALLDQVTGMNPDPDKHSEYFAVEPKL-GVPIDVAGRFQFNVYVEP 399

Cameo1  404: VWG-TSINNVILPDPDTM-VPMFWFRQELQVTPEYAHMARVALA-LRYYTPY--ALYTLTV 458
Cameo2  400: -SDHITLYENMPR---MLFPVFWVEQKAKIDPKIISELRTVRGILD-WGPTFCACFAVV- 453

Cameo1  459: IGVVLILVGVVVLIRRLLNSSDTTPLIEESA-SQ-ENQQ----- 495
Cameo2  454: IAL-L-VTAITCCTKRTEYTRPHDLL-KPYEKPKDEAEMKLNPI 494
```

C

	double-pass	single-pass
		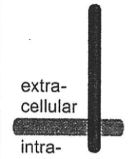
Cameo1	70 %	29 %
Cameo2	5 %	95 %
SR-BI (human)	32 %	68 %
SR-BI (mouse)	35 %	65 %
CD36 (human)	93 %	7 %
NinaD	84 %	15 %
Santa maria	97 %	3 %

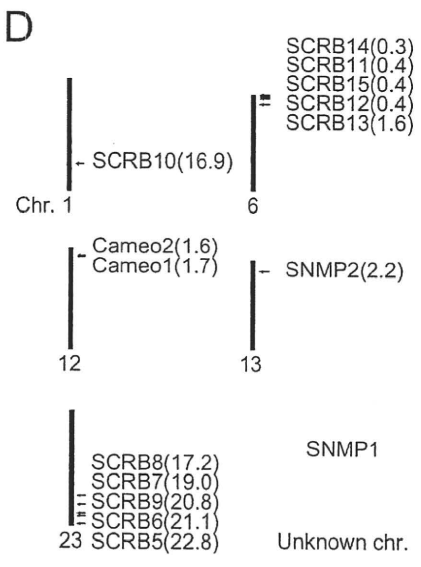

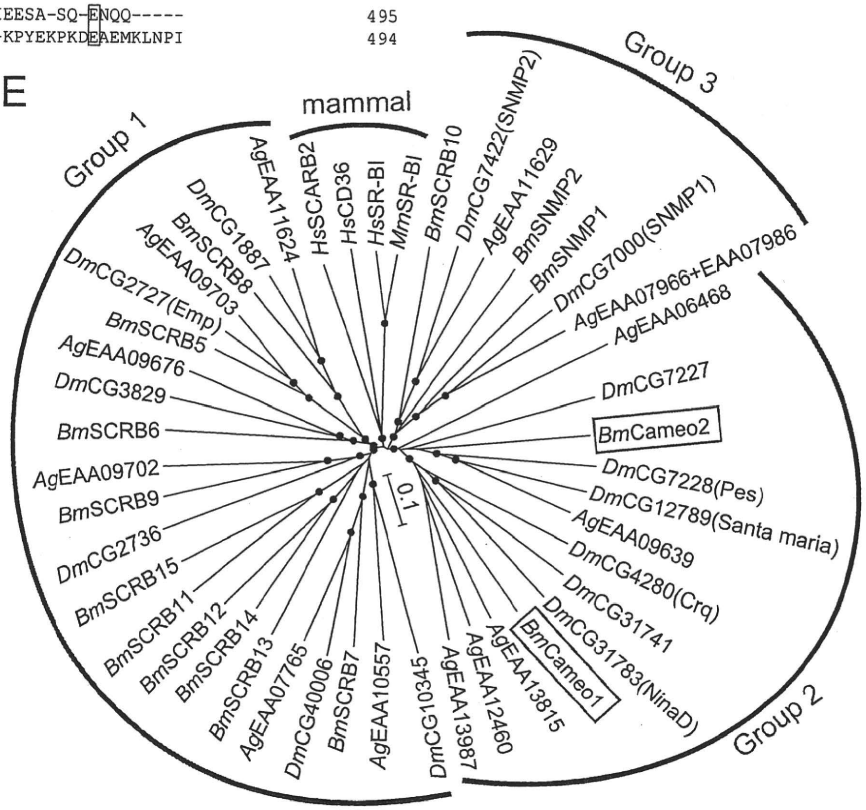

(from lysine to asparagine at amino acid position 315; K315N) was found in all of the $+^C$ allele strains and three nonsynonymous mutations in Cameo2 (V124A, V293I, and S431L) were found in part of the *C* allele strains.

Expression of Cameo2 Was Significantly Reduced in the Middle Silk Gland of the $+^C$ Allele Strain—We next examined *Cameo1* and *Cameo2* expression in the middle silk gland with multiple *C* and $+^C$ allele strains by Northern blotting analysis. With probes for *Cameo1*, no specific signal has yet been detected (data not shown). Using a ^{32}P-labeled riboprobe for *Cameo2*, one significant signal of relatively large size (>6.5 kb) and another weaker signal of smaller size (≈3.5 kb) were obtained in *C* allele strains on day 0 of the wandering stage (W0), when the larvae exhibit a characteristic behavior with enhanced locomotory activity just before spinning cocoons in the fifth instar (Fig. 4*A*). The signals were significantly reduced in each of the $+^C$ allele strains. The *Cameo2* signal in the FL501 [$+^Y$, *C*] strain, in which the hemolymph and silk gland were colorless due to the homozygous $+^Y$ allele, was not reduced to the level of the $+^C$ allele strains, suggesting that *Cameo2* expression was controlled by the *C* locus rather than lutein accumulation in the middle silk gland.

To examine protein expression of Cameo2, we prepared a rabbit polyclonal antibody for a 14-residue peptide in the predicted extracellular region that shows a low sequence similarity to Cameo1 (Fig. 3*B*). This antibody recognized a protein of ≈68 kDa in the membrane fraction of the silk gland of the *C* allele strain, but not in the $+^C$ allele strain (Fig. 4*B*), consistent with Northern blotting analysis (Fig. 4*A*). The difference between the observed and predicted molecular masses of Cameo2 (56.0 kDa in the double-pass transmembrane model and 52.7 kDa in the single-pass transmembrane model) may be due to post-translational glycosylation at asparagine residues (Fig. 3*B*). Differences between the observed and predicted molecular masses have been observed in other CD36 family genes (5). Immunohistochemistry demonstrated that the immunoreactivity for the antibody was found on the apical surface of the middle silk gland (Fig. 4*C*), which would have direct contact with the hemolymph.

Developmental and Regional Expression Profiles of Cameo1, Cameo2, and CBP in the Middle Silk Gland—Lutein pigmentation in the middle silk gland of the *C* allele strain is known to be under developmental regulation, whereas the $+^C$ allele strain remains colorless (8, 54) (Fig. 5*A*). To examine the relationship with lutein accumulation, the developmental profiles of *Cameo1* and *Cameo2* mRNA expression in the middle silk glands of both the *C* and $+^C$ allele strains were analyzed by quantitative RT-PCR from day 0 to 3 of the fourth instar (IV0-IV3) and from day 0 to 7 or 8 of the fifth instar (V0–V7 or -V8) (Fig. 5*B*). In the *C* allele strain, the expression of *Cameo1* and *Cameo2* reached a small peak on IV2, declined to a low level around the time of molting between the fourth and fifth instars, and then increased and peaked again in the middle-late fifth instar. The degree of increase in *Cameo2* expression during the fifth instar was remarkably high, showing an approximate 500-fold difference between V0 and V5. This significant increase in *Cameo2* expression during the fifth instar was consistent with the increment of the pigmentation from V3 or V4 (Fig. 5*A*). On V7, the day before pupation, *Cameo2* expression decreased markedly from V6, whereas *Cameo1* expression remained elevated. This drop in *Cameo2* expression was consistent with the loss of requirement of pigmentation for cocoon coloration because the larvae had stopped spinning and the silk gland was undergoing degradation. In the $+^C$ allele strain, the developmental profile of *Cameo1* expression was similar to that of the *C* allele strain, suggesting that the *C* locus does not largely affect *Cameo1* expression in the middle silk gland. In contrast, *Cameo2* expression was significantly lower than that observed in the *C* allele strain on all days, with a small peak on V3–V5. The lower level of *Cameo2* expression was consistent with the Northern and Western blotting analyses (Fig. 4) and the reduced degree of pigmentation in the fifth instar (Fig. 5*A*).

We separated the middle silk gland of the *C* allele strain at W0 into five sections (Fig. 5*C*), and examined *Cameo1* and *Cameo2* expression in each section by quantitative RT-PCR (Fig. 5*D*). *Cameo2* expression was significantly higher in the middle three sections than in the anterior and posterior sections, likely consistent with localization of pigmentation (Fig. 5*C*). *Cameo1* expression was relatively uniform.

We examined *CBP* expression by means of quantitative RT-PCR using the same mRNA samples employed for the above experiment. *CBP* expression was definitely repressed in the fourth instar, and increased and peaked in the fifth instar similar to *Cameo2* (Fig. 5*B*). The highest degrees on V2–V4 were consistent with the previous Western blot analysis (13). In the middle silk gland of the *C* allele strain at W0, *CBP* expression was repressed in the anterior section similar to *Cameo2*, but at a high level in the posterior section in contrast to *Cameo2* (Fig. 5*D*).

The C Locus Regulates Cameo2 Expression Likely in a cis-Regulatory Manner—To determine the molecular mechanism by which the *C* locus regulates *Cameo2* expression, we investigated whether the difference of *Cameo2* expression between the *C* and $+^C$ allele is controlled by a *cis*-regulatory element (*i.e.* expression is controlled by a non-coding element such as a

FIGURE 3. **Characteristics of the gene structures of *Cameo1* and *Cameo2*.** *A*, schematic genomic structure. *Connected dotted lines* indicates the structures of the mRNAs. *B*, alignment of putative amino acid sequences of Cameo1 and Cameo2 from the N4 strain. Transmembrane helices predicted by TMHMM version 2.0 (45) are highlighted. *N*-Glycosylation consensus sites (N-*X*-S/T) and cysteine residues in the putative extracellular region, common features in CD36-related genes (64), are indicated by *asterisks* and *bold type*, respectively. The site used to produce the antibody against Cameo2 is indicated by a *dotted underline*. The probable cleavage sites of the signal peptide predicted by the SignalP 3.0-HMM program (46) are indicated by *arrows*. *C*, hypothetical membrane topology of Cameo1, Cameo2, and other homologs predicted by TMHMM version 2.0 and SignalP 3.0-HMM. *D*, the chromosomal locations of the paralogs of *Cameo1* and *Cameo2* in the silkworm. Recently, partial sequences of *Cameo1* and *Cameo2* were reported by data base searches and named *SCRB3* and *SCRB4*, respectively (25). *E*, a neighbor-joining tree for Cameo1, Cameo2, and other homologs from insects and mammals. The first two characters of the gene names represent their species: *Bm*, *B. mori*; *Dm*, *D. melanogaster*; *Ag*, *Anopheles gambiae*; *Hs*, *Homo sapiens*; and *Mm*, *Mus musculus*. Bootstrap values >90%, based on 1000 replicates, are indicated by *closed circles*.

Cameo2 Is Coordinated with CBP in Carotenoid Transport

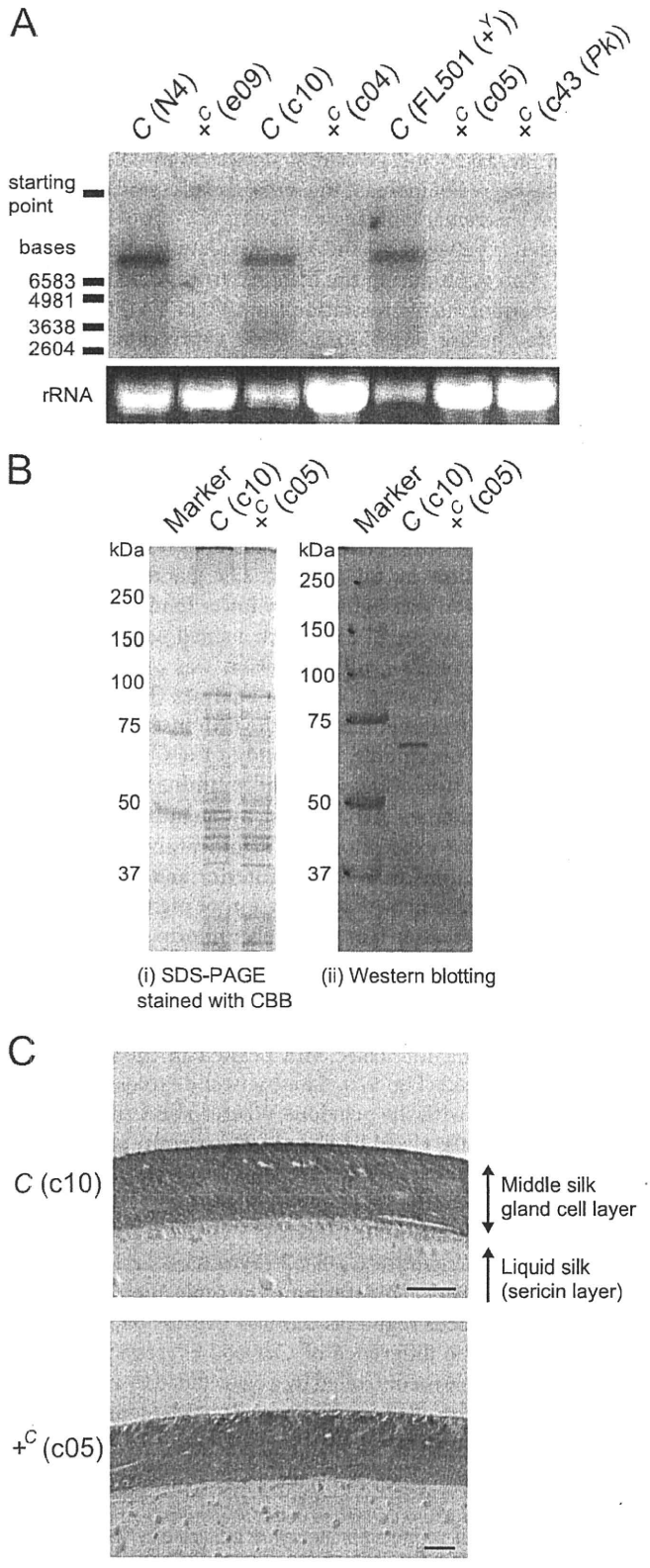

FIGURE 4. **The expression of Cameo2 was definitively repressed in the $+^C$ allele strain.** *A*, Northern blotting analysis of *Cameo2* expression in the middle silk gland at W0. *B*, SDS-PAGE and Western blotting analysis of Cameo2 from the membrane fraction of the middle silk gland at W0. *C*, immunohistochemistry of Cameo2 with the cross-section of the middle silk gland at W0. The *dark red* stains of Cameo2 were found all around the apical surface of the middle silk gland. The *blue stains* are nuclei. *Scale bar*, 20 μm.

transcriptional factor binding site) or a *trans*-acting factor (*i.e.* a coding sequence translated to a protein, such as a transcription factor). We examined SNPs of *Cameo2* mRNA in the middle silk gland of F1 individuals from the cross between the *C* and $+^C$ allele strains. In a *cis*-regulatory mechanism, *Cameo2* would be transcribed dominantly from the chromosome derived from the *C* allele strain (Fig. 6*A*). On the other hand, in a *trans*-acting mechanism, the translated products would act on *Cameo2* genes of both chromosomes from the *C* and $+^C$ allele strains, and *Cameo2* would be transcribed from both chromosomes (Fig. 6*A*). SNP analysis showed that *Cameo2* mRNA was transcribed dominantly from the *C* allele-harboring chromosome in F1 individuals, whereas *Cameo1* mRNA was transcribed from both chromosomes (Fig. 6*B*). Thus, repression of *Cameo2* expression in the $+^C$ allele strain would be controlled by a *cis*-regulatory mechanism.

The C Locus Affects Cameo2 Expression and Carotenoid Accumulation in a Tissue-specific Manner—To examine the tissue specificity of regulation of *Cameo2* expression by the *C* locus, tissue distribution of *Cameo2* was analyzed by Northern blotting (Fig. 6*C*) and RT-PCR (Fig. 6*D*) in the *C* and $+^C$ allele strains. *Cameo2* was expressed in tissues other than the middle silk gland, such as the midgut, testis, ovary, and brain, which was largely unaffected by the *C* gene. As mentioned before, the midgut, testis, and ovary also express CBP in the *Y* allele strain (12, 13). Then, carotenoid pigmentation of the testis and ovary were compared between the *C* and $+^C$ allele strains. In contrast to the difference in the middle silk gland, carotenoid pigmentation of the testis (Fig. 6*E*) and ovary (Fig. 6*F*) were similar between the *C* and $+^C$ allele strains in the background of the *Y* allele. Thus, regulation of *Cameo2* expression and carotenoid accumulation by the *C* locus appeared to be specific for the middle silk gland. Furthermore, carotenoid pigmentation in each tissue seemed to reflect both Cameo2 and CBP expression.

Restoration of Lutein Accumulation by Germ line Transformation with the Cameo2 Gene—To verify the function of Cameo2 as a product of the *C* gene, we examined the restoration of lutein accumulation in the middle silk gland after transgenic expression of the *Cameo2* gene in a strain with the phenotype of yellow hemolymph and white cocoons. The binary *GAL4/UAS* system (30) was used. An effector vector that carried the *Cameo2* gene linked to *UAS* was constructed (Fig. 7*A*) and then the effector UAS-Cameo2 (UAS) lines were generated by germ line transformation. Male moths of a UAS line were crossed with females of the Ser1-GAL4 (GAL4) line that drives target gene expression in the middle silk gland (31). The restoration of pigmentation in the middle silk gland was observed in the GAL4/UAS line (Fig. 7*B*). HPLC analysis of carotenoid content revealed the restoration of selective lutein uptake in the middle silk gland of the GAL4/UAS line (Fig. 7, *C* and *D*). Southern blotting analysis confirmed integration of the *Cameo2* transgene into the UAS line (supplemental Fig. S3*A*). RT-PCR analysis also confirmed an increase in *Cameo2* expression in the middle silk gland of the GAL4/UAS line (supplemental Fig. S3*B*). The GAL4/UAS line produced yellowish colored cocoons, whereas the intensity of coloration was weak (Fig. 7*E*).

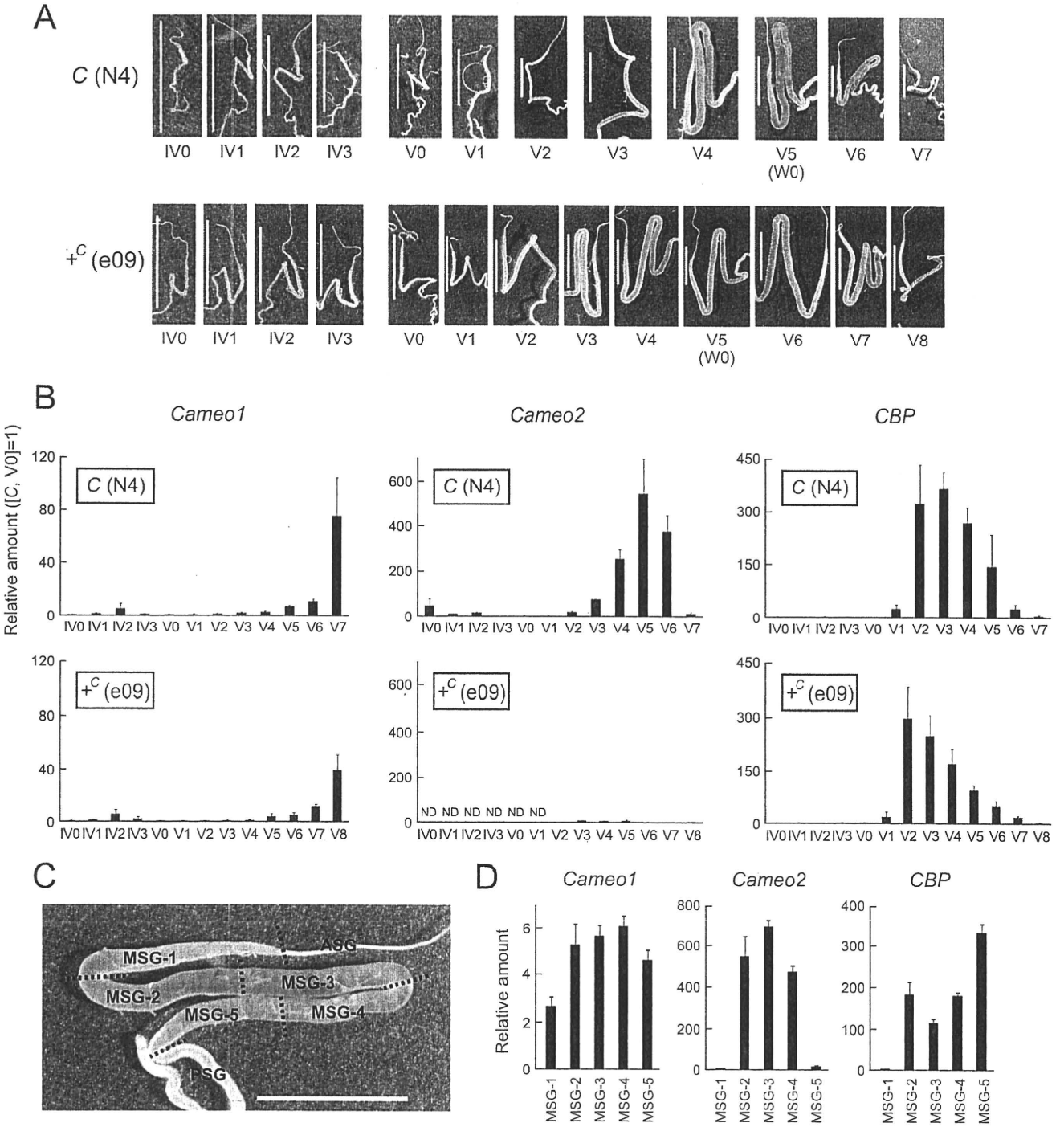

FIGURE 5. **Spatiotemporal analysis of the expression of *Cameo1* and *Cameo2* in the middle silk gland by quantitative RT-PCR.** *A*, changes in carotenoid pigmentation in the silk gland during the fourth and fifth male instars. From V5 (W0), larvae spat silk for cocoon formation, resulting in a decrease of pigmentation in the *C* allele strain. *B*, developmental expression analysis of *Cameo1*, *Cameo2*, and *CBP* in the male middle silk gland. Each *vertical axis* indicates the fold-increase in mRNA expression compared with that of the *C* allele strain at V0 (mean, S.E.; $n = 3$). *ND*, not detected. *C*, cutting lines and definition of regions in the middle silk gland for the expression analysis in *D*. The cutting lines were set at the boundary between the anterior silk gland (*ASG*) and the middle silk gland (*MSG*), the first bend, the midpoint between the first and second bend; the second bend, the midpoint between the second bend and the boundary between the MSG and the posterior silk gland (PSG), and the boundary between the MSG and the PSG. The presented silk gland of the *C* allele strain at the stage of V5 (W0) is the same as in *A*. The pigmentation in MSG-1 can derive from the posterior regions because liquid silk in the core layer of the middle silk gland likely migrates toward ASG (see the less pigmentation in MSG-1 at V4 of the *C* allele strain *A*). *D*, spatial expression analysis of the middle silk gland. Each *vertical* axis indicates the fold-increase in mRNA expression compared with that of the *C* allele strain at V0 as in *B* (mean, S.E.; $n = 3$). The stage was V5 (W0). The same data in *B* and *D* in the logarithmic scale are shown in supplemental Fig. S5. *Scale bar*, 1 cm. *Error bars* are S.E.

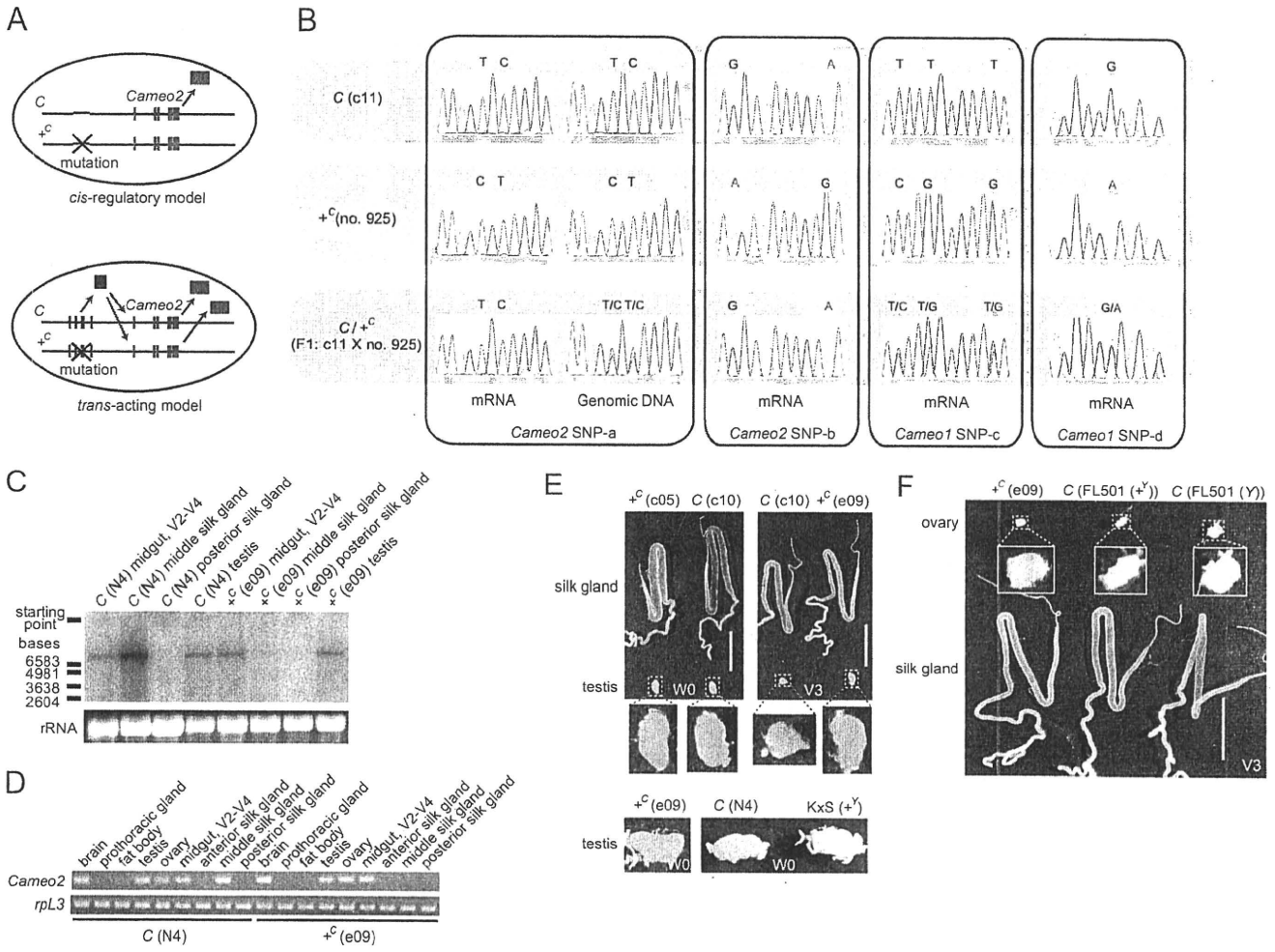

FIGURE 6. **The *C* locus controlled the *Cameo2* expression in a tissue-specific manner likely by a *cis*-regulatory manner.** *A*, schematic diagram of the principle of SNP analysis in F1 to elucidate whether *Cameo2* expression is controlled in a *cis*-regulatory or *trans*-acting manner. *B*, SNP analysis in *Cameo1* and *Cameo2* of the *C*, $+^C$, and F1 larvae. mRNA and genomic DNA were from the middle and posterior silk glands, respectively. The stage was V2–V4. The SNP sites are indicated in supplemental Fig. S2. Similar SNP patterns were obtained from three individuals of F1 larvae. *C* and *D*, examination of tissue distribution of *Cameo2* by Northern blotting (*C*) and RT-PCR (*D*) analyses. *rpL3* is an internal control (28). The stage was W0 unless otherwise noted. *E* and *F*, comparison of carotenoid pigmentation in the silk gland, testis, and ovary between the *C* and $+^C$ allele strains. Stages are indicated on the figures. *White* around the testis or ovary were fat body. *Scale bar*, 1 cm.

DISCUSSION

Recent improvements in the assembly of genome sequences (22) and physical marker resources (32, 33, 55) have made it feasible to clone mutant genes via positional cloning methods in the silkworm. Using these facilities, we attempted to elucidate the molecular identity of the *C* gene, a classical cocoon-color mutant gene mediating the cellular uptake of lutein in coordination with the *Y* gene in the middle silk gland (Fig. 1). Two paralogous membrane-spanning protein genes belonging to the CD36 gene family, *Cameo1* and *Cameo2*, were then cloned from the narrowed 375-kb interval of the *C*-linked region (see Figs. 2 and 3). Based on expression analysis (see Figs. 4 and 5) and transgenic rescue of the phenotype (see Fig. 7), the *C* gene is considered to encode Cameo2 and control the cellular uptake of lutein in the middle silk gland by regulating Cameo2 expression at a transcriptional level. The nucleotides responsible for the *C* mutation may correspond to a *cis*-regulatory element of *Cameo2*, which controls *Cameo2* expression in the middle silk gland in a specific manner (Fig. 6).

Based on the results presented here, along with those of previous studies of CBP, we propose a hypothetical transport pathway for lutein in the *C* and $+^C$ allele strains (see Fig. 7*F*). In the larval body of the *C* allele strain with the background of the *Y* allele, *Cameo2* is expressed in the midgut, middle silk gland, ovary, and testis. CBP is also expressed in these tissues (12, 13). Dietary mulberry leaves containing lutein are digested in the midgut lumen. Lutein is then absorbed into the midgut cells, possibly by Cameo2, and binds to CBP in the midgut cell to diffuse in the cytosol, which in turn transfers it to lipophorin in the hemolymph. Lipophorin reaches the middle silk gland and the genital organs via hemolymph, and then binds to the lipophorin receptor on each tissue. The lipophorin receptor on these tissues would be Cameo2 itself, another membrane receptor such as the vertebrate very low density lipoprotein receptor-like protein (56), or their complexes. Lutein is transported into these tissues by a membrane lutein transporter, which could be Cameo2 itself, where it binds to CBP in the cytosol again, resulting in yellow coloration of these tissues. In the $+^C$ allele strain

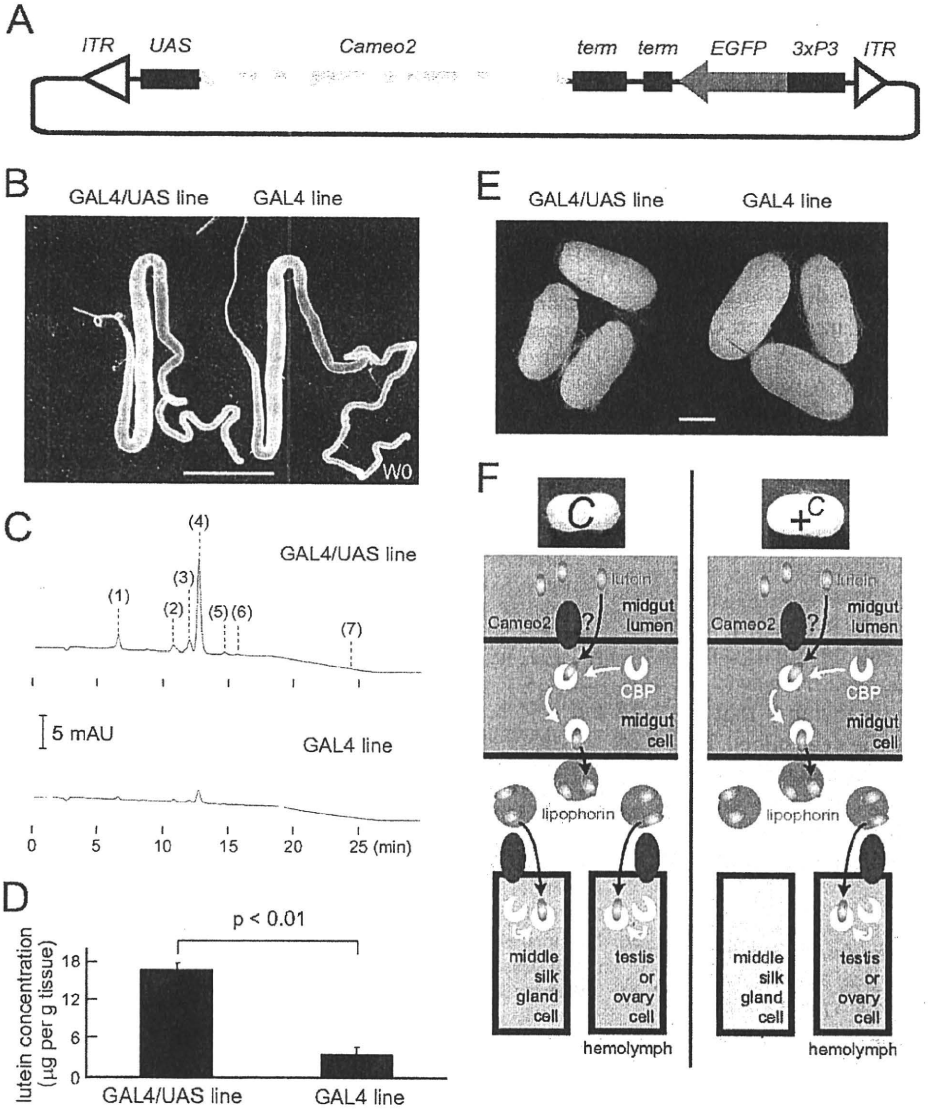

FIGURE 7. **Restoration of the phenotype of lutein accumulation by transgenic expression of *Cameo2*.** *A*, organization of the transgenic vector used. *ITR*, inverted terminal repeats of *piggyback*; *term*, SV40 terminator, *3xP3*, eye-specific promoter. *B*, silk glands of the GAL4/UAS (Ser1-GAL4/UAS-Cameo2) line, which was supposed to express Cameo2 in the middle silk gland by the binary system (30), and the GAL4 line as a control. The stage was W0. We confirmed similar stronger colorations in the GAL4/UAS line than the GAL4 line by observation of eight larvae of the GAL4/UAS line and 10 larvae of the GAL4 line. *C*, a representative chart of the reverse-phase HPLC analysis of carotenoid composition of the middle silk gland in the transgenic larvae. The stage was W0. Detection was at 474 nm. Peak positions 1, 2, 3, 4, 5, 6, and 7 correspond to the elution of 3′-dehydrolutein, 13-*cis*-lutein, unknown lutein derivative, lutein (trans lutein), zeaxanthin, 9-*cis*-lutein, and β-carotene, respectively. β-Carotene was barely detectable in the middle silk gland of the GAL4/UAS line. *D*, lutein concentration in the middle silk gland of the GAL4/UAS line and the GAL4 line (mean, S.E.; $n = 3$). The stage was W0. Statistical significance ($p < 0.01$) was analyzed by Student's *t* test. *E*, cocoon colors of the GAL4/UAS and GAL4 lines. All individuals analyzed in *B–E* exhibited the yellow hemolymph. *Scale bar*, 1 cm. *F*, model of the transport pathway for lutein in the larvae of the *C* and $+^C$ allele strains. Lutein is transported into the tissues where both Cameo2 and CBP express. Cameo2 in the internal organs would act as the lipophorin receptor and/or the membrane lutein transporter. See "Discussion" for details.

with the background of the *Y* allele, lutein would be similarly transferred to lipophorin and absorbed into the genital organs, whereas the middle silk gland rarely accumulates lutein due to its low level of Cameo2 expression. As both the CD36 family genes and the START domain-containing genes are prevalent in animals, coordination between them could also occur in other systems of selective lipid transport, as presumed for the mammalian steroidogenic system (36).

Although the midgut expresses both *Cameo2* and CBP, its feature in the cellular absorption of carotenoids is different from that of the middle silk gland as the midgut absorbs a certain amount of β-carotene in addition to lutein (8, 9). Although the present data do not deny the involvement of Cameo2 in the carotenoid absorption of the midgut, there would be other mechanisms/factors than those of the middle silk gland.

The function of Cameo1 remains elusive. Although the present results do not exclude the possibility that Cameo1 is involved in the cellular uptake of lutein, detection of *Cameo1* expression in broad tissues (see Figs. 5*D* and supplemental S4) implies that Cameo1 may be associated with a more ubiquitous function rather than tissue-specific control of lutein accumulation. It is noteworthy that tandem arrays of several paralogous genes of the CD36 gene family such as *Cameo1* and *Cameo2* are frequently observed in the silkworm (Fig. 3*D*) and Dipterans (48), whereas the physiological meaning of these tandem arrays is unknown.

Historically, the *C* mutant was originally found to produce white cocoons even though the color of hemolymph is yellow (57, 58). This was in contrast to the belief at that time that cocoon color is inevitably correlated with hemolymph color. The genetic mechanism of cocoon coloration by carotenoids has been investigated for biological and commercial purposes in part because cocoon-color genes are useful genetic markers for breeding that do not require sophisticated equipment, and cocoon colors impart distinctive color traits on some kinds of silk production. The present study identifies *Cameo2* as a molecular genetic tool for regulating cocoon color; however, the intensity of cocoon pigmentation by transgenic expression of *Cameo2* might not be enough to generate a convenient phenotype for breeding or commercial value (Fig. 7*E*). The weakness of coloration could, at least in part, be due to low uptake of lutein in the middle silk gland (Fig. 7*D*), which was 5–10-fold lower than that of the native *C* allele strain at W0 (data not shown). We expect that development of a more efficient

expression system for the transgene product in the middle silk gland would enhance the intensity of transgenic cocoon color.

Our results demonstrate that in one mutant of a membrane protein, the *Cameo2* mutant, lutein uptake of the middle silk gland is affected. One possible explanation for these observations is that Cameo2 is in the lutein-specific transfer factor present at the cell surface of the middle silk gland, which transports lutein from extracellular lipophorin to the intracellular CBP. A number of questions, however, remain. First, it is not yet known whether there are direct interactions between lipophorin and Cameo2 or Cameo2 and CBP. Although CLAMP (59), a PDZ domain-containing cytosolic protein, fatty acid-binding protein (60), and Src family proteins (61) have been suggested to have a physical interaction with the cytosolic region of SR-BI or CD36, they show no significant homology to CBP. Second, the site at which the selectivity for lutein is determined remains elusive. As the *Y* gene is involved in absorption of both lutein and β-carotene from the midgut lumen into midgut cells (8, 9) and combination of the *Y* gene and the *Flesh* gene, another cocoon-color mutant gene, facilitates the selective uptake of β-carotene in the posterior part of the middle silk gland (8, 62), the selectivity for lutein can be expected to be determined solely by Cameo2. However, the molecular properties of this CD36 family member that are responsible for lipid selectivity have yet to be determined. Biochemical and histological approaches with the *C* and *Y* mutants to these questions may reveal mechanisms by which dietary carotenoids are selectively transported to target tissues by relays of multiple factors to perform their diverse physiological functions.

Acknowledgments—We thank members of the Insect Genome Research Unit at National Institute of Agrobiological Sciences for technical assistance in the sampling of BF1 individuals for mapping and R. O. Ryan for critical reading of the manuscript.

REFERENCES

1. Goodwin, T. W. (1986) *Annu. Rev. Nutr.* **6,** 273–297
2. Loane, E., Nolan, J. M., O'Donovan, O., Bhosale, P., Bernstein, P. S., and Beatty, S. (2008) *Surv. Ophthalmol.* **53,** 68–81
3. Goldberg, I. J. (1996) *J. Lipid Res.* **37,** 693–707
4. Brown, M. S., and Goldstein, J. L. (1986) *Science* **232,** 34–47
5. Krieger, M. (1999) *Annu. Rev. Biochem.* **68,** 523–558
6. Oku, M. (1934) *Bull. Agric. Chem. Soc. Jap.* **10,** 1258–1262
7. Manunta, C. (1937) *Arch. Zool. Ital.* **24,** 385–401
8. Nakajima, M. (1963) *Bull. Fac. Agric. Tokyo Univ. Agric. Technol.* **8,** 1–80
9. Tsuchida, K., Katagiri, C., Tanaka, Y., Tabunoki, H., Sato, R., Maekawa, H., Takada, N., Banno, Y., Fujii, H., Wells, M. A., and Jouni, Z. E. (2004) *J. Insect Physiol.* **50,** 975–983
10. Van der Horst, D. J., and Ryan, R. O. (2004) in *Comprehensive Insect Physiology, Biochemistry, Pharmacology and Molecular Biology* (Gilbert, L. I., Iatrou, K., and Gill, S., eds) pp. 225–246, Elsevier, Oxford
11. Tazima, Y. (1964) *The Genetics of the Silkworm*, LOGOS Press, United Kingdom
12. Tabunoki, H., Sugiyama, H., Tanaka, Y., Fujii, H., Banno, Y., Jouni, Z. E., Kobayashi, M., Sato, R., Maekawa, H., and Tsuchida, K. (2002) *J. Biol. Chem.* **277,** 32133–32140
13. Tsuchida, K., Jouni, Z. E., Gardetto, J., Kobayashi, Y., Tabunoki, H., Azuma, M., Sugiyama, H., Takada, N., Maekawa, H., Banno, Y., Fujii, H., Iwano, H., and Wells, M. A. (2004) *J. Insect Physiol.* **50,** 363–372
14. Hara, W., Sosnicki, S., Banno, Y., Fujimoto, H., Takada, N., Maekawa, H., Fujii, H., Wells, M. A., and Tsuchida, K. (2007) *J. Insect Biotechnol. Seric.* **76,** 149–154
15. Sakudoh, T., Tsuchida, K., and Kataoka, H. (2005) *Biochem. Biophys. Res. Commun.* **336,** 1125–1135
16. Sakudoh, T., Sezutsu, H., Nakashima, T., Kobayashi, I., Fujimoto, H., Uchino, K., Banno, Y., Iwano, H., Maekawa, H., Tamura, T., Kataoka, H., and Tsuchida, K. (2007) *Proc. Natl. Acad. Sci. U.S.A.* **104,** 8941–8946
17. Alpy, F., and Tomasetto, C. (2005) *J. Cell Sci.* **118,** 2791–2801
18. Tsuchida, K., Arai, M., Tanaka, Y., Ishihara, R., Ryan, R. O., and Maekawa, H. (1998) *Insect Biochem. Mol. Biol.* **28,** 927–934
19. Harizuka, M. (1948) *J. Seric. Sci. Jap.* **17,** 1–5
20. Fujimoto, N. (1949) *J. Seric. Sci. Jap.* **18,** 82–87
21. Sturtevant, A. H. (1915) *Am. Nat.* **49,** 42–44
22. The International Silkworm Genome Consortium (2008) *Insect Biochem. Mol. Biol.* **38,** 1036–1045
23. Mita, K., Morimyo, M., Okano, K., Koike, Y., Nohata, J., Kawasaki, H., Kadono-Okuda, K., Yamamoto, K., Suzuki, M. G., Shimada, T., Goldsmith, M. R., and Maeda, S. (2003) *Proc. Natl. Acad. Sci. U.S.A.* **100,** 14121–14126
24. Rogers, M. E., Krieger, J., and Vogt, R. G. (2001) *J. Neurobiol.* **49,** 47–61
25. Tanaka, H., Ishibashi, J., Fujita, K., Nakajima, Y., Sagisaka, A., Tomimoto, K., Suzuki, N., Yoshiyama, M., Kaneko, Y., Iwasaki, T., Sunagawa, T., Yamaji, K., Asaoka, A., Mita, K., and Yamakawa, M. (2008) *Insect Biochem. Mol. Biol.* **38,** 1087–1110
26. Vogt, R. G., Miller, N. E., Litvack, R., Fandino, R. A., Sparks, J., Staples, J., Friedman, R., and Dickens, J. C. (2009) *Insect Biochem. Mol. Biol.* **39,** 448–456
27. Larkin, M. A., Blackshields, G., Brown, N. P., Chenna, R., McGettigan, P. A., McWilliam, H., Valentin, F., Wallace, I. M., Wilm, A., Lopez, R., Thompson, J. D., Gibson, T. J., and Higgins, D. G. (2007) *Bioinformatics* **23,** 2947–2948
28. Niwa, R., Sakudoh, T., Namiki, T., Saida, K., Fujimoto, Y., and Kataoka, H. (2005) *Insect Mol. Biol.* **14,** 563–571
29. Tamura, T., Thibert, C., Royer, C., Kanda, T., Abraham, E., Kamba, M., Komoto, N., Thomas, J. L., Mauchamp, B., Chavancy, G., Shirk, P., Fraser, M., Prudhomme, J. C., and Couble, P. (2000) *Nat. Biotechnol.* **18,** 81–84
30. Imamura, M., Nakai, J., Inoue, S., Quan, G. X., Kanda, T., and Tamura, T. (2003) *Genetics* **165,** 1329–1340
31. Tatematsu, K. I., Kobayashi, I., Uchino, K., Sezutsu, H., Iizuka, T., Yonemura, N., and Tamura, T. (September 30, 2009) *Transgenic Res.* 10.1007/s11248-009-9328-2
32. Yamamoto, K., Narukawa, J., Kadono-Okuda, K., Nohata, J., Sasanuma, M., Suetsugu, Y., Banno, Y., Fujii, H., Goldsmith, M. R., and Mita, K. (2006) *Genetics* **173,** 151–161
33. Yamamoto, K., Nohata, J., Kadono-Okuda, K., Narukawa, J., Sasanuma, M., Sasanuma, S. I., Minami, H., Shimomura, M., Suetsugu, Y., Banno, Y., Osoegawa, K., de Jong, P. J., Goldsmith, M. R., and Mita, K. (2008) *Genome Biol.* **9,** R21
34. Azhar, S., and Reaven, E. (2002) *Mol. Cell. Endocrinol.* **195,** 1–26
35. Martinez, L. O., Perret, B., Barbaras, R., Tercé, F., and Collet, X. (2007) in *High Density Lipoproteins* (Fielding, C. J., ed) pp. 307–338, Wiley-VCH Verlag GmbH & Co. KGaA, Weinheim
36. Connelly, M. A. (2009) *Mol. Cell. Endocrinol.* **300,** 83–88
37. Rodrigueza, W. V., Thuahnai, S. T., Temel, R. E., Lund-Katz, S., Phillips, M. C., and Williams, D. L. (1999) *J. Biol. Chem.* **274,** 20344–20350
38. Kiefer, C., Sumser, E., Wernet, M. F., and Von Lintig, J. (2002) *Proc. Natl. Acad. Sci. U.S.A.* **99,** 10581–10586
39. Voolstra, O., Kiefer, C., Hoehne, M., Welsch, R., Vogt, K., and von Lintig, J. (2006) *Biochemistry* **45,** 13429–13437
40. Wang, T., Jiao, Y., and Montell, C. (2007) *J. Cell Biol.* **177,** 305–316
41. van Bennekum, A., Werder, M., Thuahnai, S. T., Han, C. H., Duong, P., Williams, D. L., Wettstein, P., Schulthess, G., Phillips, M. C., and Hauser, H. (2005) *Biochemistry* **44,** 4517–4525
42. Reboul, E., Abou, L., Mikail, C., Ghiringhelli, O., André, M., Portugal, H., Jourdheuil-Rahmani, D., Amiot, M. J., Lairon, D., and Borel, P. (2005) *Biochem. J.* **387,** 455–461
43. During, A., Doraiswamy, S., and Harrison, E. H. (2008) *J. Lipid Res.* **49,** 1715–1724

44. Moussa, M., Landrier, J. F., Reboul, E., Ghiringhelli, O., Coméra, C., Collet, X., Fröhlich, K., Böhm, V., and Borel, P. (2008) *J. Nutr.* **138,** 1432–1436
45. Sonnhammer, E. L., von Heijne, G., and Krogh, A. (1998) *Proc. Int. Conf. Intell. Syst. Mol. Biol.* **6,** 175–182
46. Emanuelsson, O., Brunak, S., von Heijne, G., and Nielsen, H. (2007) *Nat. Protoc.* **2,** 953–971
47. Gruarin, P., Thorne, R. F., Dorahy, D. J., Burns, G. F., Sitia, R., and Alessio, M. (2000) *Biochem. Biophys. Res. Commun.* **275,** 446–454
48. Nichols, Z., and Vogt, R. G. (2008) *Insect Biochem. Mol. Biol.* **38,** 398–415
49. Franc, N. C., Heitzler, P., Ezekowitz, R. A., and White, K. (1999) *Science* **284,** 1991–1994
50. Philips, J. A., Rubin, E. J., and Perrimon, N. (2005) *Science* **309,** 1251–1253
51. Benton, R., Vannice, K. S., and Vosshall, L. B. (2007) *Nature* **450,** 289–293
52. Jin, X., Ha, T. S., and Smith, D. P. (2008) *Proc. Natl. Acad. Sci. U.S.A.* **105,** 10996–11001
53. Su, X., and Abumrad, N. A. (2009) *Trends Endocrinol. Metab.* **20,** 72–77
54. Fujimoto, N. (1943) *J. Seric. Sci. Jap.* **14,** 276–282
55. Miao, X. X., Xub, S. J., Li, M. H., Li, M. W., Huang, J. H., Dai, F. Y., Marino, S. W., Mills, D. R., Zeng, P., Mita, K., Jia, S. H., Zhang, Y., Liu, W. B., Xiang, H., Guo, Q. H., Xu, A. Y., Kong, X. Y., Lin, H. X., Shi, Y. Z., Lu, G., Zhang, X., Huang, W., Yasukochi, Y., Sugasaki, T., Shimada, T., Nagaraju, J., Xiang, Z. H., Wang, S. Y., Goldsmith, M. R., Lu, C., Zhao, G. P., and Huang, Y. P. (2005) *Proc. Natl. Acad. Sci. U.S.A.* **102,** 16303–16308
56. Gopalapillai, R., Kadono-Okuda, K., Tsuchida, K., Yamamoto, K., Nohata, J., Ajimura, M., and Mita, K. (2006) *J. Lipid Res.* **47,** 1005–1013
57. Ishii, K. (1917) *Sakurakai Zasshi.* **1,** 113–115
58. Uda, H. (1919) *Genetics* **4,** 395–416
59. Ikemoto, M., Arai, H., Feng, D., Tanaka, K., Aoki, J., Dohmae, N., Takio, K., Adachi, H., Tsujimoto, M., and Inoue, K. (2000) *Proc. Natl. Acad. Sci. U.S.A.* **97,** 6538–6543
60. Spitsberg, V. L., Matitashvili, E., and Gorewit, R. C. (1995) *Eur. J. Biochem.* **230,** 872–878
61. Huang, M. M., Bolen, J. B., Barnwell, J. W., Shattil, S. J., and Brugge, J. S. (1991) *Proc. Natl. Acad. Sci. U.S.A.* **88,** 7844–7848
62. Harizuka, M. (1953) *Bull. Seric. Exp. Sta. Jap.* **14,** 141–156
63. Zhao, Y. P., Li, M. W., Xu, A. Y., Hou, C. X., Li, M. H., Guo, Q. H., Huang, Y. P., and Guo, X. J. (2008) *Insect Sci.* **15,** 399–404
64. Hoosdally, S. J., Andress, E. J., Wooding, C., Martin, C. A., and Linton, K. J. (2009) *J. Biol. Chem.* **284,** 16277–16288

Jpn. J. Infect. Dis., 63, 2010

Laboratory and Epidemiology Communications

Echinococcus multilocularis Detected in Slaughtered Pigs in Aomori, the Northernmost Prefecture of Mainland Japan

Masaaki Kimura, Akira Toukairin, Hajime Tatezaki, Seiko Tanaka, Kunihiro Harada, Junichirou Araiyama, Hiroshi Yamasaki[1], Hiromu Sugiyama[1], Yasuyuki Morishima[1], and Masanori Kawanaka[1]*

Aomori Prefectural Towada Meat Inspection Center, Aomori 034-0001; and [1]Department of Parasitology, National Institute of Infectious Diseases, Tokyo 162-8640, Japan

Communicated by Tomoyoshi Nozaki

(Accepted December 21, 2009)

Echinococcus multilocularis is a causative agent of human alveolar echinococcosis. The distribution of the parasite in Japan was thought to be limited to the northernmost insular prefecture of Hokkaido, where the Tsugaru Strait acts as a natural physical barrier against migration to Honshu, the mainland of Japan; however, in Aomori Prefecture, situated in the northernmost part of Honshu, *E. multilocularis* infection in pigs was first reported in August and December 1998, when Aomori Prefectural Towada Meat Inspection Center (Towada MIC) detected the parasite during postmortem inspections of livers from three pigs. The infected pigs had all been transported from the same piggery in Aomori, so the implication of this case was that if the pigs had been infected while being reared on the farm, then either there had been an epidemic of *E. multilocularis* in Aomori some time previously or else the infection was epidemic at that time (1). An intensive epizootiological survey of the potential definitive and intermediate hosts in the area surrounding the piggery was undertaken, revealing no infected animals (2,3). Over the subsequent decade, Towada MIC has performed postmortem inspections of 800,000–900,000 pigs annually, including animals from the same piggery, and no pigs were found to be infected with *E. multilocularis*. However, *E. multilocularis* infection was again confirmed in the fiscal year (FY) 2008 by Towada MIC in the livers of six pigs that were transported to a slaughterhouse in Aomori directly from Hokkaido. The details of the case are given below.

From 1999 until FY2004, no pigs infected with *E. multilocularis* were reported during the routine work of Towada MIC. In FY2005, a system for surveying and monitoring *E. multilocularis* in Aomori Prefecture was put in place as part of a domestic zoonosis survey program, and the following measures were taken to bolster the monitoring system at Towada MIC. First, macroscopic photos of the livers of pigs from Hokkaido infected with *E. multilocularis* and diagnostic criteria were to be distributed to all inspectors, and samples were to be collected from livers showing signs of infection. Second, white nodular lesions in liver samples were to be stained with hemotoxylin-eosin and/or periodic acid Shiff (PAS) stain for histological examination. Third, molecular identification was to be performed together with a pathological diagnosis. Among inspections carried out from FY2005 to FY2008 under this program, the number of pigs with liver samples displaying white nodular lesions suggestive of *E. multilocularis* infection for each year was 27, 44, 25, and 13, representing a total of 109 (Table 1). Histopathological examination of the lesions did not confirm a single case of *E. multilocularis* infection, and the whitish nodules were diagnosed as lymph follicle formation, granulomatous inflammation, interstitial hepatitis, hepatic cysts, parasitic hepatitis (probably caused by the passage of ascarid larvae), etc. In FY2008, liver tissue was analyzed in 13 cases, and *E. multilocularis* cysts with PAS-positive laminated layers were detected in six of these. All of the six cases had been transported directly from Hokkaido. The cysts had obviously disrupted in the liver tissues, and neither brood capsules nor protoscoleces were observed in any of the investigated lesions. These pathological findings (Fig. 1) were consistent with those previously described in spontaneously infected pigs in Hokkaido (4). For the positive specimens, molecular confirmation of the causative agents was performed based on the method of Yamasaki et al. (5). Briefly, genomic DNAs from ethanol-fixed samples were prepared using a DNeasy Blood & Tissue kit (Qiagen, Hilden, Germany), and DEXPAT (TaKaRa Bio, Shige, Japan) was used for formalin-fixed and paraffin-embedded sections. Mitochondrial cytochrome *c* oxidase subunit 1 gene (*cox1*) was amplified by PCR. Samples for direct sequencing were prepared using an ABI PRISM BigDye Terminator Cycle Sequencing Ready Reaction kit (Applied Biosystems, Foster City, Calif., USA), and sequencing was performed on an ABI PRISM 3100-*Advant* Genetic Analyzer (Applied Biosystems). Sequence data were analyzed using EditSeq and MegAlign software (DNASTAR, Madison, Wis., USA). We amplified ~1.7 kb *cox1* in ethanol-fixed specimens,

Table 1. Number of pig postmortem inspections and results of *E. multilocularis* tests at Aomori Prefectural Towada Meat Inspection Center

	FY2005	FY2006	FY2007	FY2008	Total
Total no. of inspections	888,450	885,430	893,884	910,130	3,577,894
No. of pigs from Hokkaido	0	900	1,256	3,135	5,291
Whitish nodules in the liver	27	44	25	13	109
Positive for *E. multilocularis*	0	0	0	6	6

*Corresponding author: Mailing address: Department of Parasitology, National Institute of Infectious Diseases, Toyoma 1-23-1, Shinjuku-ku, Tokyo 162-8640, Japan. Tel: +81-3-5285-1111, Fax: +81-3-5285-1173, E-mail: mkawan@nih.go.jp

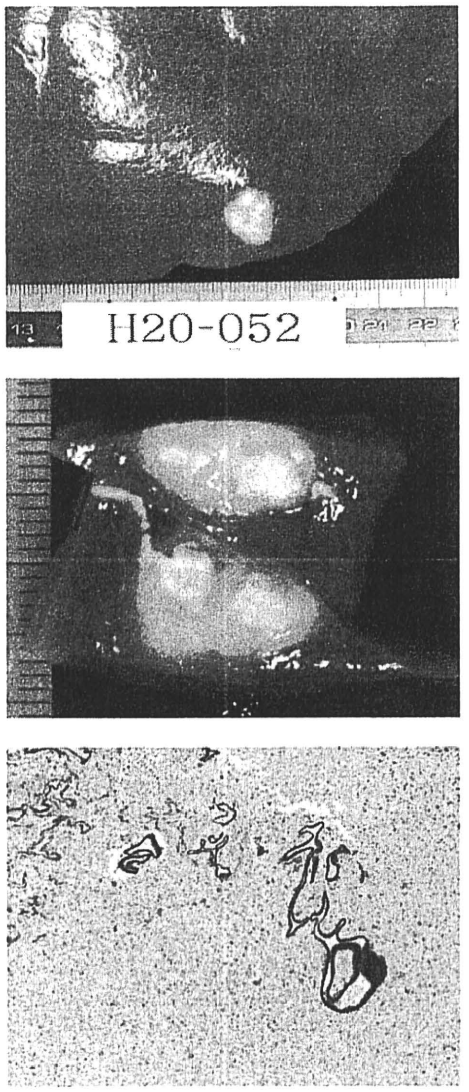

Fig. 1. Pathological findings of a hepatic echinococcal nodule. (A) Macroscopic appearance of a whitish nodule caused by *E. multilocularis*. (B) Cut surface of a nodule. (C) Magnification of a nodule showing regressive cyst of *E. multilocularis*. The cuticular layer of the cyst was strongly PAS positive. PAS stained. ×40.

and shorter sizes of *cox1* fragments (108–110 bp) were successfully amplified in formalin-fixed specimens (data not shown). DNA sequencing of the amplicons confirmed that the causative agents was *E. multilocularis* in all cases, with identical nucleotide sequences to that of *E. multilocularis* isolates from Hokkaido (GenBank accession no. AB018440).

The majority of cases of human alveolar echinococcosis in Japan have occurred in Hokkaido (approximately 500 cases to date), where *E. multilocularis* is recognized as indigenous. Approximately 80 cases of alveolar echinococcosis have been encountered in other prefectures, of which a quarter have been reported from Aomori Prefecture. Moreover, in nine of these cases there is a strong possibility that infection occurred within the prefecture (6). This is believed to be a result of the closeness with which people and goods circulate between Hokkaido and Aomori, although the specific factors responsible for infection are not known. Given this situation, the fact that *E. multilocularis* was detected in 1998 in pigs that were believed to have come from Aomori gave rise to the strong suspicion that the parasite had established its life cycle within the area. However, this could not be determined for certain; although the infected pigs were all transported from the same piggery in Aomori, the piggery in question not only bred pigs but also possessed pigs that had been purchased at livestock markets (1). The fact that in the present survey *E. multilocularis* infection was not found in pigs from outside Hokkaido suggests that there is at present a very low probability that *E. multilocularis* has established its life cycle in Aomori Prefecture. Data obtained from an inspection of 26,380,171 pigs in Hokkaido between 1983 and 2007 by the prefectural government revealed that 29,344 (0.1%) were infected with *E. multilocularis*. As shown in this report, Towada MIC has examined 5,291 pigs from Hokkaido over the last 4 years, and the rate of *E. multilocularis* detection is also approximately 0.1%. Pigs do not appear to play any role in transmission of the parasite, as the metacestode develops no brood capsules or protoscoleces in the host. However, detection of swine echinococcosis can be used as an indicator for the environmental egg contamination. Aomori is just across the Tsugaru Strait from Hokkaido, where *E. multilocularis* is endemic, and we intend to make a continual contribution to monitoring and preventing the spread of *E. multilocularis* to Honshu via postmortem inspections.

This article appeared in the Infectious Agents Surveillance Report (IASR), vol. 30, p. 243–244, 2009 in Japanese.

This study was supported in part by grants for Research on Emerging and Re-emerging Infectious Diseases from the Ministry of Health, Labour and Welfare of Japan (H18-Shinko-ippan-008 and H20-Shinko-ippan-016).

REFERENCES

1. Kamiya, H. and Kanazawa, T. (1999): The first detection of *Echinococcus* infection among pigs on the main island of Japan, August 1998–Aomori. Infect. Agents Surveillance Rep., 20, 248–249 (in Japanese).
2. Kamiya, H. (2003): Present situation and its control measure of echinococcosis in Aomori, with the consideration of its transmission from Hokkaido to mainland Japan. Jpn. Med. J., 4129, 25–29 (in Japanese).
3. Morishima, Y., Sugiyama, H., Arakawa, K., et al. (2005): A coprological survey of the potential definitive hosts of *Echinococcus multilocularis* in Aomori Prefecture. Jpn. J. Infect. Dis., 58, 327–328.
4. Sakui, M., Ishige, M., Fukumoto, S., et al. (1984): Spontaneous *Echinococcus multilocularis* infection in swine in north-eastern Hokkaido, Japan. Jpn. J. Parasitol., 10, 291–296.
5. Yamasaki, H., Nakao, M., Nakaya, K., et al. (2008): Genetic analysis of *Echinococcus multilocularis* originating from a patient with alveolar echinococcosis occurring in Minnesota, in 1977. Am. J. Trop. Med. Hyg., 79, 245–247.
6. Doi, R. (1999): Search for multilocular echinococcosis in Honshu, the mainland of Japan. Infect. Agents Surveillance Rep., 20, 6 (in Japanese).

International Journal of Food Microbiology 143 (2010) 161–165

Contents lists available at ScienceDirect

International Journal of Food Microbiology

journal homepage: www.elsevier.com/locate/ijfoodmicro

Molecular identification of *Anisakis* type I larvae isolated from hairtail fish off the coasts of Taiwan and Japan

Azusa Umehara [a,b], Yasushi Kawakami [a], Hong-Kean Ooi [c,d], Akihiko Uchida [a], Hiroshi Ohmae [b], Hiromu Sugiyama [b,*]

[a] Laboratory of Parasitology, School of Life and Environmental Science, Azabu University, 1-17-71 Fuchinobe, Chuo Ward, Sagamihara City, Kanagawa 229-8501, Japan
[b] Department of Parasitology, National Institute of Infectious Diseases, 1-23-1 Toyama, Shinjuku Ward, Tokyo 162-8640, Japan
[c] Department of Veterinary Medicine, National Chung Hsing University, 250 Kuo Kuang Road, Taichung 402, Taiwan
[d] Faculty of Agriculture, Yamaguchi University, 1677-1 Yoshida, Yamaguchi City, Yamaguchi 753-8515, Japan

ARTICLE INFO

Article history:
Received 4 June 2010
Received in revised form 11 August 2010
Accepted 11 August 2010

Keywords:
Anisakis typica
Anisakis simplex sensu stricto
Anisakis pegreffii
Ribosomal DNA internal transcribed spacer
Hairtail

ABSTRACT

Anisakid nematodes are known to cause the zoonotic disease, anisakiasis, through the consumption of raw or undercooked fish. The parasites most frequently associated with the disease in humans are categorized as *Anisakis* type I, which comprise several species of the genus *Anisakis*. The larvae show primitive forms and lack the detailed morphological characteristics required for precise species identification. Thus, molecular characterization is necessary for determining the species of *Anisakis* type I larvae and acquiring important clinical and epidemiological information. In this study, we isolated *Anisakis* type I larvae from hairtail fish caught off the coasts of Taiwan and Japan. The ribosomal DNA (rDNA) internal transcribed spacer (ITS) region was sequenced, and restriction fragment length polymorphism (RFLP) analyses using *Hinf*I and *Hha*I was carried out for species identification. Most larvae isolated from hairtail caught in Taiwan were *Anisakis typica* (84%), while those isolated from hairtail caught in Japan were almost exclusively identified either as *Anisakis simplex* sensu stricto (65%) or *Anisakis pegreffii* (33%). This is the first report of *A. typica* in fish obtained from Taiwan. Our results shed the light on the epidemiology of *Anisakis* type I larvae, which is a potential cause of human anisakiasis in Taiwan and Japan.

1. Introduction

Larvae of anisakid nematodes are commonly found in marine fish and squid. Many cases of human anisakiasis caused by larvae belonging to the family Anisakidae have been reported in Japan and other countries due to the increasing popularity of eating raw fish (Lymbery and Cheah, 2007). Berland (1961) classified the larvae of anisakid nematodes into only two types, namely *Anisakis* types I and II, based on morphological characteristics such as the length of the ventriculus and presence/absence of mucron at the tip of the tail. The type I larvae were recognized as the parasite most frequently associated with human anisakiasis (Oshima, 1972; Smith and Wootten, 1978). Controversy regarding the species names of *Anisakis* type I and II larvae still remains because the larvae lack the detailed morphological characteristics required for precise species identification. The use of allozyme markers made it possible for the type I morphotypes to be identified as *Anisakis pegreffii*, *Anisakis simplex* sensu stricto, *Anisakis simplex* C, *Anisakis typica*, and *Anisakis ziphidarum* (Mattiucci et al., 1997, 2002; Paggi et al., 1998). The former three species have been recognized as sibling species belonging to *Anisakis simplex* sensu lato. The species comprising *Anisakis* types I and type II have also been characterized by sequencing and restriction fragment length polymorphism (RFLP) analyses of the ribosomal DNA (rDNA) internal transcribed spacer region (ITS region), namely the 5.8S rDNA and flanking ITS regions, ITS1 and ITS2 (Mattiucci and Nascetti, 2006, 2008). The classifications based on allozyme markers were fully consistent with the results obtained by these molecular methods.

It is imperative to identify *Anisakis* type I larvae detected in food fish in order to improve food safety. Hairtail is one of the most common and economically important food fish in the East and South China Seas. In Japan, Taiwan, and Korea, hairtail is often sold in markets and is favored for raw consumption as sashimi or sushi. However, few studies have investigated the molecular identification of anisakid larvae isolated from hairtail (Shih, 2004). Therefore, in this study, we detected *Anisakis* type I larvae in hairtail collected from Taiwan and Japan and applied these molecular methods for species identification.

2. Materials and methods

2.1. Parasite materials

Seven hairtail (*Trichiurus* spp.) specimens caught off the coast of each of the following 5 localities were examined for anisakid larvae:

* Corresponding author. Tel.: +81 3 5285 1111; fax: +81 3 5285 1173.
E-mail address: hsugi@nih.go.jp (H. Sugiyama).

0168-1605/$ – see front matter © 2010 Elsevier B.V. All rights reserved.
doi:10.1016/j.ijfoodmicro.2010.08.011

Taichung, Taiwan, and Nagasaki, Kochi, Wakayama and Shizuoka prefectures, Japan. We purchased the fish at retail fish markets in the respective localities, except for fish from Nagasaki, which were purchased from a retail fish market in Tokyo. Fish were examined immediately after transfer to our laboratory in Taichung (samples from Taiwan) or in Tokyo (samples from Japan).

Anisakid larvae were isolated from the visceral surface and body cavity of the fish. The larvae were observed under light and dissection microscopes for morphological identification (Ishii et al., 1989), and third-stage larvae of *Anisakis* type I were used for further molecular investigation.

2.2. DNA amplification

DNA samples were extracted from individual worms using a DNeasy Blood and Tissue Kit (Qiagen K. K., Tokyo, Japan) according to the manufacturer's instructions. The entire ITS region (ITS1, 5.8S rDNA and ITS2) was amplified by PCR using primers NC5 (forward; 5′-GTAGGTGAACCTGCGGAAGGATCATT-3′) and NC2 (reverse; 5′-TTAGTTTCTTTTCCTCCGCT-3′) (Abe et al., 2005). PCR was conducted using a mixed solution (5 μl) of extracted DNA as a template, with a reaction mixture (45 μl) containing 1.25 units of *TaKaRa EX Taq*, 1× PCR buffer (10 mM Tris-HCl pH 8.3, 50 mM KCl, 1.5 mM $MgCl_2$), 0.2 mM of each dNTP (Takara Bio Inc., Shiga, Japan) and 0.5 μM of each primer. PCR was performed using a LittleGene PCR machine (Bioer, Hangzhou, China) with 35 cycles as follows: denaturation at 98 °C for 5 s, annealing at 52 °C for 30 s, and extension at 72 °C for 60 s. A final extension was carried out at 72 °C for 10 min. The PCR products were separated by electrophoresis on 1.0% Seakem GTG agarose gels (Lonza Rockland, Inc., Rockland, ME, USA) in Tris-borate-EDTA buffer and visualized by illumination with short-wave ultraviolet light after ethidium bromide staining.

2.3. RFLP analysis

Restriction enzymes *Hin*fI and *Hha*I (New England Biolabs, Ipswithch, MA, USA) were used in the RFLP analysis for identifying the species of *Anisakis* type I, according to the genetic key of D'Amelio et al. (2000). The PCR products were digested according to the manufacturer's recommendations. The digested samples were then separated by electrophoresis on 2.0% Seakem GTG agarose gels (Lonza Rockland, Inc.) and visualized as previously described.

2.4. Sequencing

The PCR products were excised from the agarose gels and sequenced using a BigDye Terminator Cycle Sequencing Kit (Applied Biosystems Inc., Foster City, CA, USA) on an automated sequencer (ABI3100, Applied Biosystems). Sequence similarities were determined by a BLAST search of the DNA Data Bank of Japan (DDBJ) (http://blast.ddbj.nig.ac.jp/top-j.html). Sequence alignment and comparison was facilitated by the GENETYX-WIN program (ver.7.0, Software Development Co, Tokyo, Japan).

3. Results

3.1. Detection of Anisakis type I larvae from Taiwan and Japan

Six of the 7 hairtails from Taiwan and 15 of the 28 hairtails from Japan were positive for anisakid nematodes (Table 1), and 110 and 61 larvae were identified as *Anisakis* type I from these locations, respectively. The identification was based on the presence of a long ventriculus with an oblique ventricular-intestinal junction and a rounded tail possessing a mucron.

Table 1
Molecular identification of the *Anisakis* type I larvae.

Locality	Date of collection	No. of fish	No. of parasites			
		Infected/examined	Collected	Identified as		
				At[a]	Ap[b]	As[c]
Taiwan (Taichung)	14 Oct 2008	6/7	110	93	15	2
Japan (Nagasaki)	3 Dec 2008	5/7	20	0	20	0
Japan (Kochi)	13 Jul 2010	1/7	2	0	0	2
Japan (Wakayama)	18 Jul 2010	2/7	6	0	0	6
Japan (Shizuoka)	12 Jul 2010	7/7	33	1	0	32

[a] *A. typica*.
[b] *A. pegreffii*.
[c] *A. simplex* sensu stricto.

3.2. PCR-RFLP analysis

Amplification of the entire ITS region produced a single band of about 950 bp for all specimens. In RFLP, digestion of the PCR products with *Hin*fI produced three different RFLP patterns, corresponding to *A. typica* (ca. 590 and 330 bp), *A. pegreffii* (ca. 330, 280 and 240 bp), or *A. simplex* s. str. and *A. simplex* C (ca. 620 and 240 bp) (Fig. 1). For specimens showing the *A. simplex* s. str. and *A. simplex* C patterns, we then digested their respective PCR products only with *Hha*I and confirmed bands of ca. 530 and 420 bp for the *A. simplex* s. str. pattern (data not shown). Based on RFLP analyses of the 110 larvae from Taiwan, 93 (84%) were identified as *A. typica*, 15 (14%) were *A. pegreffii*, and 2 (2%) were *A. simplex* s. str. However, among 61 specimens from Japan, 40 (65%) were identified as *A. simplex* s. str., 20 (33%) were *A. pegreffii*, and 1 (2%) was *A. typica* (Table 1, Fig. 2).

3.3. Sequence of the entire ITS region

Entire ITS region sequences were determined for 5 larvae of *A. typica*, 5 larvae of *A. pegreffii*, and 1 larva of *A. simplex* s. str. from Taiwan as well as 1 larva of *A. typica* from Japan. No intraspecific differences were found in the sequences of these specimens. Similarity searches of the GenBank/EMBL/DDBJ nucleotide database revealed that the sequence of *A. typica* was identical to deposited sequences of the same species obtained at the larval stage from chub mackerel (*Scomber japonicus*, accession number AB432908) and at the

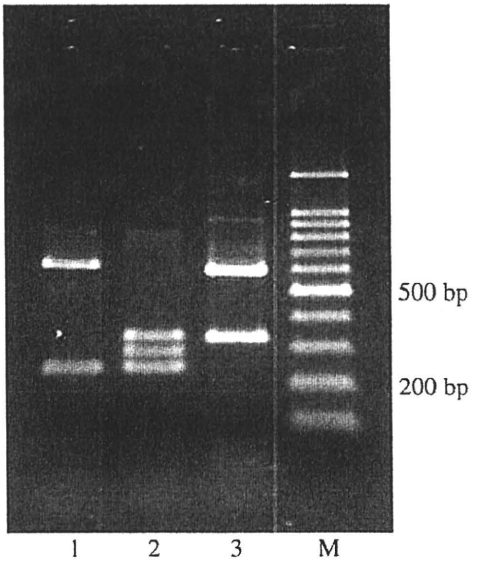

Fig. 1. RFLP analysis with *Hin*fI of the ITS PCR products amplified from the *Anisakis* type I larvae. Lane 1: *A. simplex* sensu stricto; Lane 2: *A. pegreffii*; Lane 3: *A. typica*. The 100-bp DNA ladder marker was used to estimate the size of the bands (lane M).

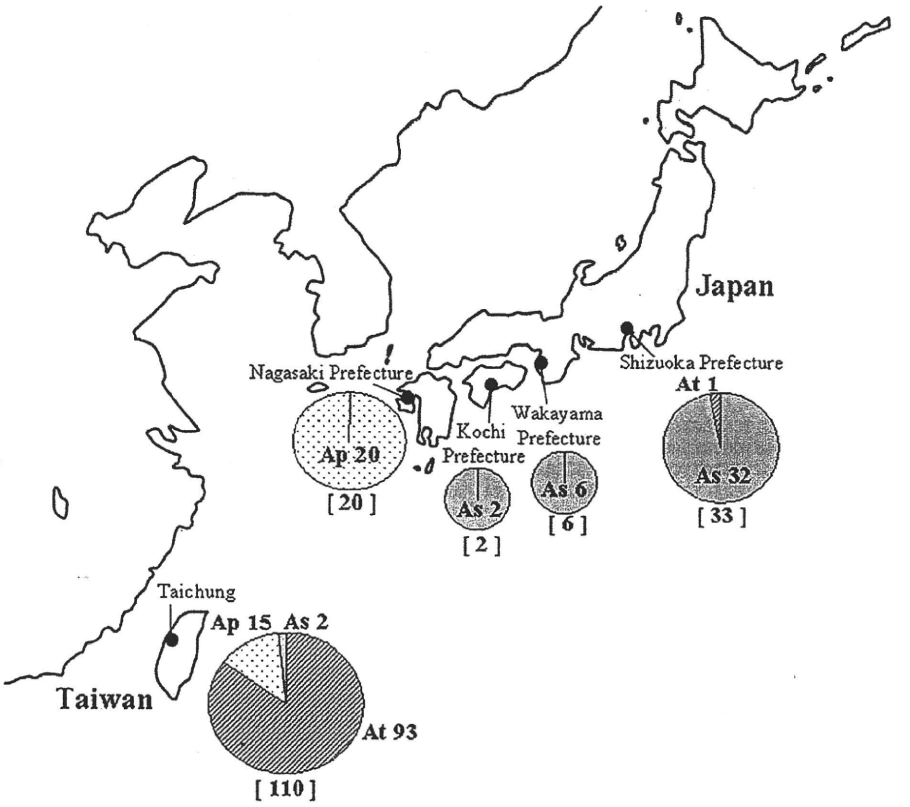

Fig. 2. Distribution of *A. typica* (At), *A. pegreffii* (Ap) and *A. simplex* sensu stricto (As) isolated from hairtail caught in coastal areas of Taiwan and Japan. Pie charts show the distribution of *Anisakis* type I larvae based on analysis of the rDNA ITS region. The numbers in square brackets and after the abbreviations of the species (At, Ap and As) represent the number of larvae examined and identified, respectively.

adult stage from rough-toothed dolphin (*Steno bredanensis*, AB479120). The nucleotide sequence of *A. typica* from Taiwan determined in this study has been deposited in the DDBJ/EMBL/GenBank database under the accession number AB551660. The sequences of *A. pegreffii* and *A. simplex* s. str. were also found to be identical to deposited sequences of each species obtained from chub mackerel (*S. japonicus*, AB277823) and arabesque greenling (*Pleurogrammus azonus*, AB277822), respectively.

The ITS sequence of *A. simplex* reported by Shih (2004) was not available from the GenBank/EMBL/DDBJ (shown in Fig. 3). Shih also isolated larvae for sequencing analysis from hairtail from Taiwan. Comparison with the sequence obtained in this study revealed that the sequence reported by Shih was 99% and 77% similar to those of *A. typica* and *A. simplex* s. str., respectively (Fig. 3).

4. Discussion

Anisakiasis is a zoonotic disease caused by the ingestion of anisakid nematodes in raw or undercooked fish. In previous reports, almost all the larvae recovered from humans have been identified as *Anisakis* type I based on their morphological characteristics (Oshima, 1972; Smith and Wootten, 1978). Since *Anisakis* type I is a morphotype comprising several species of the genus *Anisakis*, molecular characterization of *Anisakis* type I larvae is necessary for identifying each clinically and epidemiologically important species.

In this study, we observed that most of the larvae isolated from hairtail specimens from Taiwan were that of *A. typica*. To the best of our knowledge, this is the first report of *A. typica* in fish from Taiwan. In addition, a larva of *A. typica* was first detected in a hairtail specimen from Japan, though this species has been isolated from mackerel in Japan (Umehara et al., 2008a; Suzuki et al., 2010). In Asian countries besides Taiwan and Japan, *A. typica* has been reported in China, Korea, Indonesia and Thailand (Zhu et al., 2007; Chen et al., 2008; Palm et al., 2008; Lee et al., 2009; Du et al., 2010).

Shih (2004) reported the isolation of anisakid larvae from hairtail from Taiwan and sequenced the rDNA ITS region. Surprisingly, the so-called *A. simplex* sequence determined by Shih had a 99% similarity to the sequence of *A. typica* in this study. This implies that the sequence of anisakid larvae reported by Shih was probably that of *A. typica*, and not of *A. simplex*. According to the review by Mattiucci and Nascetti (2006, 2008), *A. typica* is widely distributed between 30°S and 35°N in warm and tropical waters. Nevertheless, there have been few reports of *A. typica* detected in both paratenic host fish and definitive host marine mammals. Kagei (2003) reported that the number of worms of *A. typica* in the definitive host was less than that for *A. simplex*. The lack of reports of *A. typica* might also be due to insufficient recognition of the species and hence misidentification of *A. typica* as *A. simplex*.

The sequence of *A. typica* obtained in this study was identical to the two sequences already deposited in the GenBank/EMBL/DDBJ (AB432908 and AB479120). However, when compared with the sequence reported by Shih as *A. simplex*, the *A. typica* sequence differed by 4 nucleotides in the ITS1 region and 1 nucleotide in the ITS2 region. Previous studies have reported geographical intraspecific variations in the entire ITS region of *A. typica* from Indonesia and Brazil (Palm et al., 2008, Iñiguez et al., 2009). This may indicate that some genotypes of *A. typica* are globally distributed in the ocean.

Japanese people traditionally eat fish raw as sushi and sashimi, and over 2000 cases of human anisakiasis are estimated to occur annually (Chai et al., 2005). In Taiwan, consumption of raw fish is also a common practice, and anisakiasis is therefore an important consideration. However, only one case has been reported in Taiwan to date, and the causative pathogen was not identified (Ishikura, 2003).

Fig. 3. Alignment of the entire ITS region sequences of *A. typica*. As (Shih, 2004), the sequence incorrectly reported as *A. simplex*; At (AB432908), the sequence obtained from larva isolated from chub mackerel; At (AB479120), the sequence obtained from adults isolated from rough-toothed dolphin; At (present study), the sequence obtained from larva isolated from hairtail in Taiwan in this study (AB551660). Asterisk (*) indicates identity to the reference sequence. GenBank/EMBL/DDBJ accession numbers are each shown in parentheses, where applicable.

We recently identified the species of the *Anisakis* type I larvae isolated from fish and from anisakiasis patients in Japan (Umehara et al., 2006, 2007, 2008b). Although both *A. simplex* s. str. and *A. pegreffii* were detected in fish, almost all larvae (99%) from patients were identified as *A. simplex* s. str. In other words, there is a striking discrepancy in the predominant species between fish and humans. Suzuki et al. (2010) explained that this was due to the higher penetration rate of *A. simplex* s. str. into the muscle tissue of the fish. *A. simplex* s. str. larvae were therefore ingested by humans together with the fish muscles, while *A. pegreffii* larvae were usually removed from the fish along with the internal organs prior to ingestion.

To date, although *A. typica* has not been recorded as a cause of human anisakiasis and the risk of human infection by *A. typica* has been assumed to be low, Palm et al. (2008) reported the isolation of a single larva of *A. typica* from the musculature of the bullet tuna (*Auxis rochei rochei*). Since *A. typica* is the predominant species in the hairtail